AD_____

CONTRACT NO: DAMD17-91-C-1100

TITLE: GENETIC AND PHYSIOLOGICAL STUDIES OF BACILLUS ANTHRACIS RELATED TO DEVELOPMENT OF AN IMPROVED VACCINE

PRINCIPAL INVESTIGATOR: Curtis B. Thorne

CONTRACTING ORGANIZATION: Department of Microbiology
University of Massachusetts
Amherst, Massachusetts 01003

REPORT DATE: December 31, 1992

TYPE OF REPORT: Midterm Report

PREPARED FOR: U.S. ARMY MEDICAL RESEARCH AND DEVELOPMENT COMMAND
Fort Detrick, Frederick, Maryland 21702-5012

DISTRIBUTION STATEMENT: Approved for public release;
distribution unlimited

The findings in this report are not to be construed as an official Department of the Army position unless so designated by other authorized documents.

REPORT DOCUMENTATION PAGE

Form Approved
OMB No. 0704-0188

1. AGENCY USE ONLY *(Leave blank)*	2. REPORT DATE	3. REPORT TYPE AND DATES COVERED
	31 December 1992	Midterm Report (6/30/91-12/31/92

4. TITLE AND SUBTITLE
Genetic and Physiological Studies of Bacilius Anthracis Related to Development of an Improved Vaccine

5. FUNDING NUMBERS
Contract No.
DAMD17-91-C-1100

61102A
3M161102BS12.AD.100
WUDA335909

6. AUTHOR(S)
Curtis B. Thorne

7. PERFORMING ORGANIZATION NAME(S) AND ADDRESS(ES)
Department of Microbiology
University of Massachusetts
Amherst, Massachusetts 01003

8. PERFORMING ORGANIZATION REPORT NUMBER

9. SPONSORING/MONITORING AGENCY NAME(S) AND ADDRESS(ES)
U.S. Army Medical Research & Development Command
Fort Detrick
Frederick, Maryland 21702-5012

10. SPONSORING/MONITORING AGENCY REPORT NUMBER

11. SUPPLEMENTARY NOTES

12a. DISTRIBUTION/AVAILABILITY STATEMENT
Approved for public release; distribution unlimited

12b. DISTRIBUTION CODE

13. ABSTRACT *(Maximum 200 words)*

During this reporting period most of our effort was spent on studies concerning the biology of the two *B. anthracis* plasmids, pXO1 which carries genes for anthrax toxin synthesis and pXO2 which carries genes for capsule synthesis. Transposon mutagenesis with Tn*917* was applied to both plasmids; a library of insertions mutants of each plasmid has been produced and the mutants have been analyzed by restriction analysis to determine the sites of insertion and their locations on the respective physical maps of the two plasmids. The information has led to the discovery and cloning of a gene on pXO1 that is a positive *trans*-activator of toxin synthesis. Other results from studies of insertion mutants of pXO1 suggest that a negative regulatory gene is located on the plasmid. Attempts are being made to clone the putative gene. Studies of insertion mutants of pXO2 strongly suggest that some of the mutations are located in genes(s) regulating synthesis of anthrax capsular material. Among such mutants are those that overproduce capsular material, some that no longer require bicarbonate and CO_2 for capsule synthesis, and some that have lost the ability to synthesize capsules. Attempts are in progress to clone some of these regulatory sequences.

14. SUBJECT TERMS	15. NUMBER OF PAGES
B. Anthracis; Anthrax Toxin; Protective Antigen; Plasmid pX01; Plasmid pX02; Transposon Mutagenesis; RAD I; BD; Anthrax Vaccine; Plasmids	16. PRICE CODE

17. SECURITY CLASSIFICATION OF REPORT	18. SECURITY CLASSIFICATION OF THIS PAGE	19. SECURITY CLASSIFICATION OF ABSTRACT	20. LIMITATION OF ABSTRACT
Unclassified	Unclassified	Unclassified	Unlimited

FOREWORD

Opinions, interpretations, conclusions and recommendations are those of the author and are not necessarily endorsed by the U.S. Army.

( ) Where copyrighted material is quoted, permission has been obtained to use such material.

( ) Where material from documents designated for limited distribution is quoted permission has been obtained to use the material.

(X) Citations of commercial organizations and trade names in this report do not constitute an official Department of the Army endorsement or approval of the products or services of these organizations.

( ) In conducting research using animals, the investigator(s) adhered to the "Guide for the Care and Use of Laboratory Animals", prepared by the Committee on Care and Use of Laboratory Animals of the Institute of Laboratory Animal Resources, National Research Council (NIH Publication No. 86-23, Revised 1985).

( ) For the protection of human subjects, the investigator(s) have adhered to policies of applicable Federal Law CFR 46.

(X) In conducting research utilizing recombinant DNA technology, the investigator(s) adhered to current guidelines promulgated by the National Institutes of Health.

CB Thorne 1/4/93

PI Signature Date

TABLE OF CONTENTS

Midterm Report

This is the midterm report submitted under contract DAMD17-91-C-1100. Research on the contract which began June 30, 1991 is a continuation of research previously carried out under contract DAMD17-85-C-5212.

During the eighteen months represented by this midterm report our research concentrated largely on (i) physical and genetic analysis of the *B. anthracis* toxin plasmid pXO1; and (ii) physical and genetic analysis of the *B. anthracis* capsule plasmid pXO2. A very small proportion of our effort was also directed toward development of the bacteriophage TP-21 as a vector for transposon mutagenesis.

In this report our main efforts for the past eighteen months are described and discussed following a general description of materials and methods. Specific procedures which themselves are results of the research are described as appropriate under individual sections.

Materials and Methods

Organisms. Table 1 lists the bacterial strains and plasmids referred to in this report.

Media. For convenience to the reader, compositions of the various culture media referred to in this report are given below. All amounts are for one liter final volume. For preparation of solid medium, 15 grams of agar (Difco) were added per liter of the corresponding broth.

NBY broth: Nutrient broth (Difco), 8 g; Yeast extract (Difco), 3 g.

Phage assay (PA) broth: Nutrient broth (Difco), 8 g; NaCl, 5 g; $MgSO_4.7H_2O$, 0.2 g; $MnSO_4.H_2O$, 0.05 g; $CaCl_2.2H_2O$, 0.15 g. The pH was adjusted to 6.0 with HCl.

Phage assay agar: For bottom agar, 15 g of agar were added per liter of phage assay broth. For soft agar, 0.6 g of agar were added per liter.

L broth: Tryptone (Difco), 10 g; Yeast extract (Difco), 5 g; NaCl, 10 g. The pH was adjusted to 7.0 with NaOH.

LPA agar: L agar containing the salts of PA broth.

$LPACO_3$ agar: LPA agar with 5 g of $NaHCO_3$.

LG broth: L broth with 1 g of glucose.

BHI broth: Brain heart infusion broth (Difco), 37 g.

Peptone diluent: Peptone (Difco), 10 g. Used for diluting phage and bacterial cells.

Minimal I: $(NH_4)_2SO_4$, 2 g; KH_2PO_4, 6 g; K_2HPO_4, 14 g; sodium citrate, I g; glucose, 5 g; L-glutamic acid, 2 g; $MgSO_4.7H_20$, 200 mg; $FeCl_3.6H_2O$, 40 mg; $MnSO_4.H_2O$, 0.25 mg. The pH was adjusted to 7.0 with NaOH. The glucose and $FeCl_3$ were sterilized separately.

Minimal IB: The basal medium is the same as Minimal I except that $FeSO_4$ (14 mg) is substituted for $FeCl_3$ and $MnSO_4 \cdot H_2O$ is increased to 12.5 mg. The following are added: thiamine hydrochloride, 10 μg; and 160 μg each of L-methionine, L-leucine, L-valine, L-alanine, L-serine, L-threonine, L-proline, and L-phenylalanine.

Minimal IC: Minimal I with 5 g of vitamin-free Casamino acids (Difco) and 10 mg of thiamine hydrochloride.

Minimal XO: To Minimal 1 are added 10 mg of thiamine hydrochloride, 200 mg of glycine, and 40 mg of L-methionine, L-serine, L-threonine, and L-proline.

CA broth is the Casamino acids medium as described by Thorne and Belton (20).

CA-agarose medium: CA-agarose medium for the detection of colonies producing protective antigen was prepared as follows: 0.75 g of agarose was added to 100 ml of CA broth, prepared as described by Thorne and Belton (20), and the mixture was steamed until the agarose was dissolved. When the medium cooled to about 50° C, 1 ml of 20% glucose, 8 ml of 9% $NaHCO_3$, 6 ml of goat antiserum to *B. anthracis* and 10 ml of horse serum were added. The medium was dispensed in petri plates (13 ml per plate) and the plates were left with their lids ajar while the agarose solidified. The plates were usable after 1 hr.

Quantitative determination of PA, LF, and EF. In some instances, the culture filtrates were concentrated 2- to 40-fold by ultrafiltration in Centricon 30 microconcentrator units (Amicon, Beverly, MA). The amount of PA and LF in the sample filtrates were determined by a radial immunodiffusion assay. The radial immunodiffusion agarose medium consisted of 1% Seakem GTG agarose (FMC BioProducts, Rockland, ME), 2% polyethylene glycol 8000, 3% fetal bovine serum, 20 mM HEPES (pH 7.5), 0.15 M NaCl, 2 mM EDTA, 0.025% sodium azide, and either 0.5% goat antiserum to PA or 0.7% rabbit antiserum to LF (supplied by S. Leppla). A well approx. 2.5 mm in diameter was cut into the agarose medium and 8 μl of the filtrate was added to each well. Each plate included a set of standards containing 5 to 50 μg of purified PA or LF (supplied by S. Leppla) per ml. The diameter of the precipitin ring was measured and the data were compared to a standard curve.

EF in the culture filtrates was determined by an adenylate cyclase assay according to a method described by Leppla (6). A set of standards containing 0.05 to 1 μg of purified EF (supplied by S. Leppla) per ml was included in each assay. Briefly, approx. 10 μl of sample filtrate or purified EF standard were mixed with 40 μl of a reaction mixture containing 50 mM HEPES (pH 7.5), 12.5 mM $MgCl_2$, 2.5 mM dithiothreitol, 1.25 mM $CaCl_2$, 1.25 mM EDTA, 1.25 mM ATP, 0.25 mM cyclic AMP, 2.5 mg of bovine serum albumin, fraction V per ml, 25 μg of calmodulin (Sigma Chemical Co., St. Louis, MO) per ml, and 1.25 μCi of α-^{32}P-ATP per ml. The reactions were incubated for 10 min. at room temperature. The reactions were stopped by adding 100 μl of a stopping solution containing 1% SDS, 50 mM ATP, and 1.25 mM cyclic AMP. Approx. 1 ml of distilled water was added to each tube.

The radiolabelled cyclic AMP product was separated from the nonreacted radiolabelled ATP reactant by sequential chromatography on cation exchange and aluminum oxide (Alumina) columns. The reaction mixtures were poured over Dowex AG 50W-X4 (200-400 mesh) columns that had been washed previously with 2 X 8 ml of distilled water. When the mixtures had drained into the columns, the columns were washed twice with 1.5 ml of distilled water to elute the nonreacted radiolabelled ATP. Any radiolabelled material left on the column was eluted with 5 ml of distilled water directly onto neutral Alumina WN-3 columns which had been washed previously with 8 ml of 0.1 M Imidazole (pH 7.3). Once the effluent from the Dowex 50 columns had drained into the Alumina columns, the radiolabelled cyclic AMP was eluted with 6 ml of 0.1 M Imidazole (pH 7.3) directly into 7-ml scintillation vials. The sample effluents were then counted in a Beckman LS5000 TD scintillation counter. The Dowex 50 columns were recycled by washing them twice with 2 ml of 1 M HCl and the Alumina columns were recycled by washing them with 3 ml of 0.1 M Imidazole (pH 7.3). The data obtained for the culture filtrates was compared to a standard curve prepared for purified EF.

Transfer of DNA to nylon membranes. DNA electrophoresed on an agarose gel was transferred to a Magnagraph nylon membrane (Micron Separations Inc., Westboro, MA) using a modified method of that described by Boehringer Mannheim Corp. (Technical Update (Nov. 1990), Indianapolis, IN). The DNA in the gel was acid nicked by incubation in 0.25 N HCl for 10 to 15 min. The gel was rinsed in distilled water and placed in 0.5 N NaOH-1.5 M NaCl for 30 min. with gentle agitation to denature the DNA. The gel was then neutralized in 1.5 M NaCl-1.0 M Tris-HCl (pH 8.0) for 1 h with gentle agitation. The DNA was blotted from the neutralized gel onto a Magnagraph nylon membrane by capillary transfer using 10X SSC for 12 to 16 h. After the transfer, the membrane was gently washed in 6X SSC for 5 min., air dried for 1 h, and then baked at 80^{o}C in a vacuum oven for 1 to 2 h. The membrane was either used immediately for hybridization or stored in a dry place for use later.

Labelling probe DNA with digoxygenin-11-dUTP. Digoxygenin-11-dUTP was incorporated into the probe DNA by random primer labelling according to a method described for nonradioactive labelling of DNA by Boehringer Mannheim Corp. (Indianapolis, IN). The hexanucleotide mixture, digoxygenin DNA labelling mixture, and the Klenow fragment were purchased from Boehringer Mannheim Corp. The reaction was carried out in a final volume of 50 μl in a 1.5-ml microcentrifuge tube. The probe DNA was denatured by placing the DNA solution in a boiling water bath for 10 min. and then quickly chilling the solution for 3 min. in an ice/ethanol bath. Each reaction mixture contained approx. 1 to 3 μg of denatured DNA, 5 μl of hexanucleotide mixture, 5 μl of digoxygenin DNA labelling mixture, and enough sterile distilled water to bring the volume to 47.5 μl. DNA synthesis was started by adding 2.5 μl of Klenow fragment. The reactants were gently mixed and placed in a 37^{o}C water bath for 16 to 20 h.

To terminate the reaction, 5 μl of 0.2 M disodium EDTA (pH 8.0) was added to the reaction mixture. The labeled DNA was precipitated with 1 μl of a glycogen solution (20 mg/ml), one-tenth volume of 4 M LiCl, and 3 volumes of 100% ethanol. The precipitation was carried out for 4 to 6 h at -20°C. The labeled DNA was collected by centrifugation and the DNA pellet was washed once with 70% ethanol. A dry DNA pellet was then resuspended in 50 μl of TE (10 mM Tris-HCl, 1 mM disodium EDTA, pH 7 to 8) containing 0.1% SDS for 10 min. at 37°C. Prior to hybridization, the digoxygenin-labelled DNA probe was denatured in prehybridization solution by heating in a boiling water bath for 10 min. and chilling the mixture quickly in an ice/ethanol bath for 3 min.

DNA-DNA hybridization. DNA-DNA hybridizations were done according to a method described by Boehringer Mannheim Corp. for nonradioactive DNA labelling and detection. The Magnagraph nylon membrane containing the immobilized DNA was prehybridized in a sealed plastic bag at 68°C for 1 to 3 h in 20 ml of freshly prepared 5X SSC solution containing 0.1% (w/v) sodium N-lauroylsarcosine, 0.02% (w/v) SDS, and 1% (w/v) Genius blocking reagent (Boehringer Mannheim) per 100 cm^2 of membrane. After prehybridization, the solution covering the membrane was replaced with 2.5 ml of prehybridization solution containing 250 ng to 1 μg of denatured digoxygenin-labelled DNA probe per 100 cm^2 of membrane. The bag was sealed and the hybridization was continued at 68°C for 16 to 24 h.

The membrane was removed from the hybridization solution, washed twice in 2X SSC containing 0.1% SDS for 5 min. at room temperature, and washed twice in 0.1X SSC containing 0.1% SDS for 15 min. at 68°C with gentle shaking. The hybridized DNA probe was detected on the membrane by chemiluminescence.

Chemiluminescent detection of hybridized DNA. The method for detecting the hybridized DNA probe with Lumi-Phos 530 solution was described by Boehringer Mannheim Corp. After post-hybridization washes, the membrane was equilibrated for 1 min. in Buffer A (100 mM Tris-HCl, 150 mM NaCl, pH 7.5). The membrane was transferred to Buffer B (Buffer A containing 2% (w/v) Genius blocking reagent) for 3 h with gentle shaking. The membrane was then transferred to 30 ml of a 1 to 5000 dilution of an anti-digoxygenin alkaline phosphatase antibody conjugate (diluted in Buffer B) per 100 cm^2 of membrane. The membrane was incubated in this solution for 30 min. with gentle shaking. After the 30-min. incubation, the membrane was washed two times for 15 min. in Buffer A and then equilibrated for 2 min. in Buffer C (100 mM Tris-HCl, 100 mM NaCl, 50 mM $MgCl_2$, pH 9.5). Finally, the membrane was placed on a clean sheet of acetate film with DNA side up and 2 to 3 ml of Lumi-Phos 530 (Boehringer Mannheim Corp.) was placed directly onto the membrane. A second sheet of acetate film was placed on top of the filter to spread the solution evenly over the membrane. The reaction was allowed to proceed for 15 to 30 min. before the membrane (placed in a sealed bag) was exposed to X-ray film (Kodak XAR film). The membrane was

exposed to the X-ray film for 1 to 30 min. and the X-ray film was developed according the instructions provided by the manufacturer.

Isolation of pBluescriptIIKS+. The pBluescriptIIKS+ was isolated from *E. coli* DH5α(pBluescriptIIKS+) by a modification of a boiling lysis method (9). Twelve ml of an overnight culture of *E. coli* DH5α(pBluescriptIIKS+) grown in L broth containing 100 μg of ampicillin per ml was centrifuged at 10,000 rpm for 10 min. The pellet was resuspended in 0.7 ml of 8% sucrose/5% triton X-100/50 mM EDTA/50 mM Tris-HCl (pH 8) and the suspension was transferred to a 1.5-ml microcentrifuge tube. Fifty μl of a freshly prepared 10 mg/ml solution of lysozyme in 0.25 M Tris-HCl (pH 8) was added to the cell suspension and the mixture was placed in a boiling water bath for 1 min. The lysed mixture was centrifuged for 15 min. at room temperature and the cell debris was removed with a sterile toothpick. Ten μl of a RNAse solution (10 mg/ml) was added to the supernatant and placed at 37^{O}C for 15 min. An equal volume of a 1:1 mixture of phenol-chloroform was added to the tube and gently mixed. The mixture was centrifuged to separate the phases. The aqueous layer was transferred to a fresh tube and the phenol-chloroform extraction was repeated until no white interface was detected (usually 4 to 7 extractions). The final extraction was with an equal volume of 24:1 chloroform-isoamyl alcohol mixture.

The DNA was precipitated with 0.15 volume of 7.5 M ammonium acetate and an equal volume of cold isopropanol. The DNA was allowed to precipitate at -20^{O}C for 20 min. The precipitated DNA was then recovered by centrifugation in a refrigerated microcentrifuge at 13,000 rpm for 30 min. The pellet was washed with 1 ml of cold 70% ethanol. The DNA was then allowed to air dry for 1 h and resuspended in 100 μl of TE (10 mM Tris-HCl, 1 mM EDTA, pH 8.0).

Preparation of vector for ligation. Approximately 20 μg of plasmid DNA was digested to completion with an excess amount of restriction endonuclease. The DNA was precipitated overnight at -20^{O}C with one-tenth volume of 3 M sodium acetate (pH 5.2) and 2 volumes of 95% ethanol. The DNA was collected by centrifugation in a refrigerated microcentrifuge at 13,000 rpm for 30 min. and washed with 1 ml of cold 70% ethanol. The pellet was allowed to air dry and then resuspended in 50 μl of TE (pH 8). Twenty μl was frozen at -20^{O}C for use as a control in the ligation reactions.

The remaining DNA was treated with calf-intestine alkaline phosphatase (Promega Corp., Madison, WI) according to manufacturer's instructions. Briefly, the volume of the DNA suspension was brought to 40 μl with TE (pH 8). Five μl of a 10X reaction buffer containing 0.5 M Tris-HCl, pH 9, 10 mM $MgCl_2$, 1 mM $ZnCl_2$, and 10 mM spermidine and 2 μl of calf-intestine alkaline phosphatase (CIAP) were added to the DNA suspension. The mixture was placed at 37^{O}C for 30 min. Another 2 μl of CIAP was added to the mixture and again placed at 37^{O}C for 30 min. The reaction was stopped by the addition of 300 μl of 10 mM Tris-HCl, pH 7.5/1 mM EDTA, pH 7.5/200 mM NaCl/0.5% SDS. The mixture was placed at 60^{O}C for 15 min. The DNA was then extracted with phenol-chloroform and the aqueous phase was precipitated with

0.5 volume of 7.5 M ammonium acetate and 2 volumes of 95% ethanol. The precipitated DNA was collected by centrifugation, allowed to air dry, and finally resuspended in a total volume of 50 μl TE (pH 8).

Elution of DNA fragments. Restriction fragments were isolated by agarose gel electrophoresis and the elution of the fragments was carried out using an Elutrap electroseparation chamber according to the manufacturer's instructions (Schleicher and Schuell, Inc., Keene, NH). The elution was run at 200 V for 2 to 3 h and the DNA was collected in 400 to 500 μl of 1X Tris-borate buffer. The DNA was then precipitated with one-tenth volume of 3 M sodium acetate (pH 5.2) and 2 volumes of 100% ethanol. The DNA was collected by centrifugation in a microcentrifuge at 4^{o}C for 30 min. The DNA pellet was dried for 30 min. at room temperature and resuspended in 50 ul of TE.

Ligation reactions. Ligation reactions were carried out according to methods described by Sambrook *et. al.* (15). Vector and insert DNA were mixed at a molar ratio of 1:3 in a total volume of 10 to 20 μl. Control ligations included digested vector alone to determine if the ligation was successful and CIAP-treated digested vector alone to determine if the CIAP treatment had reduced vector religations. The concentrations of the DNA used in the control ligations were the same as that used for the vector in the vector/insert ligation mixture. The mixtures were heated to 65^{o}C for 5 min. and chilled on ice for 5 min. to melt any reannealled ends. A one-tenth volume of the 10X reaction buffer containing 300 mM Tris-HCl, pH 7.8/100 mM $MgCl_2$/100 mM DTT/10 mM ATP and 3 weiss units of T4 DNA ligase (Promega Corp., Madison, WI) were added to each tube. The mixture was ligated overnight at room temperature. The following day an additional 1 weiss unit of ligase was added to each tube and the mixture was allowed to continue ligation at room temperature. The ligation mixture was precipitated with one-tenth volume of 3 M sodium acetate (pH 5.2) and 2 volumes of 100% ethanol and dialyzed against TE (pH 8) for use in electroporation of electrocompetent *E. coli* DH5α cells and to prevent arcing in the electroporation cuvettes.

Transformation of *E. coli*. The ligation mixtures were transformed into electrocompetent cells of *E. coli* DH5α by electroporation using a GenePulser apparatus according to methods and instructions provided by the manufacturer (Bio-Rad Laboratories, Richmond, CA). Briefly, four 250-ml flasks of L broth were inoculated with 2.5 ml of an overnight culture of *E. coli* DH5α. The cultures were grown at 37^{o}C until an OD_{600} of 0.5 to 0.7 was reached. The flasks were chilled for 15 min. on ice and the cells were harvested by centrifugation. The pellets were washed one time in 1 liter and one time in 500 ml of cold sterile distilled water. Finally, the pooled pellet was washed one time in 20 ml of cold 10% glycerol. The final pellet was resuspended in 200 μl of cold 10% glycerol. The suspended electrocompetent cells were dispensed into 40 μl samples. To each sample 2 to 3 μl of the precipitated/dialyzed ligation mixture was added. The mixture was transferred to a chilled 0.2-cm electroporation cuvette and pulsed one time at 2.5 kV, 25μFD, and 200 ohm resistance. One ml of SOC medium was immediately added to the cuvette and

the cell suspension was transferred to a cotton-plugged culture tube. The cultures were incubated at 37°C with shaking for 1 h. The cultures were plated onto L agar containing 100 μg of ampicillin per ml and which had been spread 1 h before with 100 μl of 100 mM isopropylthio-ß-D-galactoside (IPTG) and 40 μl of 2% 5-bromo-4-chloro-3-indolyl-ß-D-galactoside (Xgal). The plates were incubated at 37°C for 16 to 20 h. The blue color was allowed to develop further at room temperature. The plasmids from the white Lac⁻ colonies were screened for possible inserts.

Results and Discussion

I. Physical and genetic analysis of the *B. anthracis* toxin plasmid pXO1.

As reported previously (17), Weybridge UM44 exhibited different plasmid-derived phenotypic characteristics from those observed in Weybridge A strains. (It should be recalled that the Trp⁻ auxotroph, Weybridge UM44, was isolated from the "wild-type" Weybridge strain, and Weybridge A was isolated from "wild-type" Weybridge as a mutant that grew much better than the parent strain on a minimal medium, minimal XO). The two strains, Weybridge UM44 and Weybridge A (and auxotrophs derived from the latter) differed in rate and extent of sporulation at 37°C, phage sensitivity, and growth characteristics on minimal medium. However, UM44-derived strains into which pXO1::Tn*917* derivatives from UM23 were introduced showed characteristics similar to those typical of UM23. No apparent differences were observed in *Bam*HI restriction patterns of pXO1 from Weybridge UM44 and pXO1 from Weybridge A UM23. However, there were some differences in the *Pst*I and *Eco*RI restriction patterns of pXO1 from the two strains. Two new fragments were observed in *Pst*I digests and in *Eco*RI digests of pXO1 from Weybridge UM44 compared to those of pXO1 from Weybridge A UM23. Because of differences observed in the toxin plasmid from the two strains, we have suggested that the plasmid of the wild-type Weybridge strain (and that from Weybridge UM44) be designated pXO1 and the one from Weybridge A strain be designated pXO1.1. In keeping with this convention the toxin plasmid from other *B. anthracis* strains should be designated pXO1.2, pXO1.3, etc., as they are characterized.

Characterization of Tn*917* insertion mutants. Transposon mutagenesis utilizing pTV1 has been used previously to generate Tn*917* insertions in pXO1.1 from *B. anthracis* Weybridge A UM23. Phenotypic characterization of several Tn*917* insertion mutants and the locations of Tn*917* within pXO1.1 from several of these mutants have been described previously (3, 4, 17, 18). During the period covered by this report more insertion mutants have been characterized.

As shown in Fig. 1, Tn*917* inserted into a number of different sites on pXO1.1. Construction of the restriction map of pXO1.1 will be discussed below. Several insertion mutants exhibited characteristics similar to those of the Weybridge A UM23 parent strain and these mutants are shown in Fig. 1 without a

phenotypic designation. Mutant tp28 exhibited alterations in its sensitivity to bacteriophage CP-51. Restriction analysis showed that Tn*917* inserted in the 6.6-kb *Bam*HI fragment of pXO1.1. Several insertion mutants and the deletants shown in Fig. 1 exhibited alterations in toxin production. Two insertion mutations appear to have interrupted genes involved in regulation of toxin synthesis. The mutants, tp29, tp32, and tp62, containing these insertion mutations as well as other insertion mutants and deletants have been characterized further.

Table 2 lists the altered fragments of plasmids from six mutants and the phenotypic alterations exhibited by these mutants. Mutants tp70, tp73, and tp74 exhibited deletions of approx. 16 kb within the toxin-encoding region of pXO1.1. Each of these plasmids was missing the 18.1-kb and 6.0-kb *Pst*I fragments and the 34.8-kb, 13.9-kb and 6.0-kb *Bam*HI fragments; however, new *Pst*I and *Bam*HI fragments were observed that were approx. 14.0 kb and 44.2 kb in size, respectively. These results were similar to those obtained from restriction analysis of pXO1.1::Tn*917* from tp21 (see Fig. 1). The deletions observed in the plasmids from tp21, tp70, and tp73 (tp74 may be a sibling of tp73) appear to be identical even though the insertions resulted from independent transpositional events. This evidence suggested that Tn*917* insertions in particular locations of the toxin-encoding region of pXO1.1 may promote deletions within this region.

As shown in Table 2, Tn*917* insertion in pXO1.1 from tp56 was in the 13.9-kb *Bam*HI fragment. This result was similar to that observed for pXO1.1::Tn*917* from tp29 and tp32, both of which are deficient in toxin synthesis. Mutants tp32 and tp56 were isolated from the same transposon mutagenesis experiment which suggested that they may be siblings. Tn*917* insertion in the plasmid from tp72 was in the 6.0-kb *Bam*HI fragment and the 6.0-kb *Pst*I fragment. Mutant tp68 which appears to produce PA in the absence of added bicarbonate contains Tn*917* within the 34.8-kb *Bam*HI fragment, or more precisely, in the 6.6-kb *Pst*I fragment. Results from double digestion of the plasmids from tp72 and tp68 (discussed below) showed that Tn*917* inserted within *pag* and *lef*, respectively. This is consistent with the observation that tp72 fails to produce PA; however, further characterization of tp68 will be necessary to determine whether Tn*917* insertion in the *lef* gene of pXO1.1 from this mutant is responsible for its altered PA phenotype.

Location and orientation of Tn*917* in pXO1.1 from various insertion mutants. Tn*917* insertions in the pXO1.1 derivatives from several insertion mutants and deletants were localized first by restriction analysis with *Bam*HI and *Pst*I. Then the location and orientation of Tn*917* were defined more precisely in the plasmid derivatives by double digestions with *Bam*HI and *Sal*I (Table 3). *Sal*I was chosen because it cuts pXO1.1 infrequently and it cuts Tn*917* once. The *Sal*I restriction site in Tn*917* is located almost in the middle of the transposon (25). When pXO1.1::Tn*917* is digested with *Bam*HI and *Sal*I, the *Bam*HI fragment containing Tn*917* will be cleaved into two fragments. The site of insertion can be calculated by subtracting the size of the *Sal*I arm of Tn*917* (2.6 kb) from the altered *Bam*HI-*Sal*I fragments. Tn*917* insertions in the

*Bam*HI fragments of the plasmids from tp2A, tp21, tp29, tp32, tp36, tp39, tp68, and tp72 were localized to one site based on these results and those from previous restriction analyses. Tn*917* insertions in pXO1.1 from tp20, tp27, tp40, and tp62 were localized to one of two regions within the *Bam*HI fragment; however, only the Tn*917* insertion site in the plasmid from tp62 was defined further by restriction analysis of the altered *Bam*HI-*Sal*I fragments (see below).

The orientation of Tn*917* within the altered *Bam*HI fragments could be determined by DNA-DNA hybridizations of the double-digested plasmids with the *Ava*I arms of Tn*917*. *Ava*I cleaves Tn*917* into 3 fragments approx. 2.2 kb, 1.8 kb, and 1.2 kb in size. The 2.2-kb fragment represents one end of the transposon and the 1.8-kb fragment represents the other end of the transposon which encodes the *erm* gene. These two *Ava*I fragments of Tn*917* were isolated, labelled with digoxigenin-labelled dUTP, and hybridized to the double-digested plasmids from the insertion mutants and deletants listed above.

The location and orientation of Tn*917* insertions within the toxin-encoding region of pXO1.1 from tp2A, tp27, tp29, tp32, tp36, tp62, tp 68, and tp72 are shown in Fig. 2. The construction of the restriction map of the 77-kb linear region of pXO1.1 is described below. The arrow above the insertion site shows the orientation of Tn*917* with reference to the direction of transcription of *erm*, *tnpR*, and other proposed ORFs (13). As shown in Table 3, four insertion mutations within the region of pXO1.1 depicted in Fig. 2 appeared to affect toxin production. The results showing the locations of Tn*917* within the altered 34.8-kb *Bam*HI fragment of the plasmids from tp2A, tp36, and tp62 were used to determine the order of the *Pst*I fragments within this large *Bam*HI fragment. Finally, the ends of the deletions in the plasmids from tp21 and tp39 were determined from the locations of the Tn*917* insertions within the altered *Bam*HI fragment.

Analysis of the plasmids from tp29 and tp32 showed that *Sal*I cut the altered 13.9-kb *Bam*HI fragment into two fragments, approx. 15 kb and 4.5 kb in size. Based on calculations from this data, Tn*917* inserted approx. 2 kb within the 13.9-kb *Bam*HI fragment of pXO1.1. The *Eco*RI restriction profile of the plasmids from tp29 and tp32 showed that Tn*917* inserted into an 8.0-kb *Eco*RI fragment. DNA-DNA hybridization analysis of digested pXO1.1 with radiolabelled pSE42, the recombinant plasmid containing the cloned EF structural gene, showed that pSE42 hybridized to the 7.4-kb *Bam*HI fragment and the 8.0-kb, 3.1-kb, and 1.1-kb *Eco*RI fragments of pXO1.1 (data not shown). These results provided evidence that the 8.0-kb *Eco*RI fragment links the 13.9-kb *Bam*HI fragment with the 7.4-kb *Bam*HI fragment. Thus, the transposon inserted just downstream of the EF structural gene and 2 kb within the 13.9-kb *Bam*HI fragment (Fig. 2). Hybridization analysis showed that the orientation of Tn*917* is opposite to the direction of transcription of *cya*. As shown in Table 3, tp29 and tp32 are deficient in production of the toxin components. Tn*917* insertion within the 13.9-kb *Bam*HI fragment seemed to interrupt a gene involved in positive regulation of toxin synthesis. A 2.0-kb fragment localized to this region of the *Bam*HI fragment has

been cloned and a gene designated as *atxA* has been identified whose product activates toxin synthesis (discussed below).

Analysis of the plasmid from tp72 showed that *Sal*I cut the altered 6.0-kb *Bam*HI fragment into two fragments approx. 8.2 kb and 3.2 kb in size. Based on calculations from these data and results from previous restriction analyses, Tn*917* was located approx. 0.6 kb within the 6.0-kb *Bam*HI fragment, placing the insertion within the 3' end of the PA structural gene. DNA-DNA hybridization analysis showed that the direction of transcription of Tn*917* is the same as that reported for *pag*. These results provided evidence that the $PA^{+/-}$ phenotype observed for tp72 resulted from insertion of the transposon into the *pag* gene.

Mutant tp68 was of interest because it produced a halo on CA haloimmunoassay plates both in the presence and absence of added bicarbonate and CO_2, suggesting that it could produce toxin when grown under either condition. Tn*917* was calculated to have inserted 5.1 kb within the 34.8-kb *Bam*HI fragment or approx. 0.5 kb within the 6.6-kb *Pst*I fragment of the plasmid from tp68. These results suggested that the transposon inserted into the 5' end of the LF structural gene (Fig. 2). Further characterization of tp68 will be necessary to determine whether Tn*917* insertion in the LF structural gene is responsible for its altered toxin phenotype.

Tp62 produces PA and LF in the absence of added bicarbonate and it overproduces both proteins when bicarbonate is added to the medium (4). *Bam*HI-*Sal*I restriction analysis of the plasmid from this mutant showed that *Sal*I cut the altered 34.8-kb *Bam*HI fragment into a 24-kb and 15-kb fragment. To determine the site of insertion, the 15-kb *Bam*HI-*Sal*I fragment was eluted and digested with *Pst*I. *Pst*I cut the 15-kb fragment into three fragments, 6.6 kb, 4.7 kb, and 3.4 kb in size, and correspond to the 6.6-kb, 6.0-kb, and 9.3-kb *Pst*I fragments of the 34.8-kb *Bam*HI fragment, respectively. The 34.8-kb *Bam*HI fragment hybridized to the 9.3-kb, 6.6-kb, 6.3-kb, 6.0-kb, and 5.2-kb *Pst*I fragments. Based on results from DNA-DNA hybridizations of digested pXO1.1 with the clone toxin structural genes, the PA and LF structural genes hybridized in part to the 6.0-kb *Pst*I fragment, linking the 34.8-kb *Bam*HI fragment with the 6.0-kb *Bam*HI fragment (see Fig. 2). The LF structural gene was also shown to hybridize to the 6.6-kb *Pst*I fragment, linking this fragment to the 6.0-kb *Pst*I fragment. Sequence analysis of *pag* (24) suggested that the 6.0-kb *Pst*I fragment is cut by *Bam*HI into fragments approx. 1.4 kb and 4.7 kb in size. Thus, the evidence suggested that the 4.7-kb fragment obtained by digestion of the 15-kb *Bam*HI-*Sal*I with *Pst*I is homologous to the 6.0-kb *Pst*I fragment of pXO1.1. The *Pst*I restriction profile of the plasmid from tp62 showed that Tn*917* inserted into a 9.3-kb fragment. By process of elimination, the 3.4-kb fragment obtained by *Pst*I digestion of the 15-kb *Bam*HI-*Sal*I fragment is most likely homologous to the 9.3-kb *Pst*I fragment. This would link the 9.3-kb *Pst*I fragment to the 6.6-kb *Pst*I fragment. By subtracting the size of the *Sal*I arm of Tn*917* (2.6 kb) from the 3.4-kb fragment, the site of the Tn*917* insertion was calculated to be approx. 0.8 kb within the 9.3-kb *Pst*I fragment. The location of the insertion is just upstream of the LF

structural gene (Fig. 2), suggesting that this region may be involved in negative regulation of toxin synthesis. We are currently trying to clone this region to determine whether a gene encoding a trans-acting factor is located within this *Pst*I fragment (discussed below). The direction of transcription of Tn*917* within the 9.3-kb fragment is the same as that of the LF structural gene.

Double digestion of the plasmids from tp2A and tp36 showed that Tn*917* appeared to have inserted into the same site on these plasmids. *Sal*I, in both instances, cut the altered 34.8-kb *Bam*HI fragment into two fragments approx. 30 kb and 9.5 kb in size. *Eco*RI and *Pst*I restriction profiles of the plasmids from tp2A and tp36 showed that Tn*917* inserted into the same 1.1-kb *Eco*RI fragment, but it inserted into the 5.2-kb *Pst*I fragment of the plasmid from tp2A and into the 6.3-kb *Pst*I fragment of the plasmid from tp36. The results obtained from these restriction analyses were not useful in linking the 5.2-kb and 6.3-kb *Pst*I fragments to the 9.3-kb *Pst*I fragment within the 34.8-kb *Bam*HI fragment. Previous restriction analysis of transductionally-shortened pXO1.1::Tn*917* derivatives from UM23C1 tds1, tds2, and tds6, and tds9 provided evidence that determined the order of these *Pst*I fragments in the large *Bam*HI fragment. The results showed that the plasmids from all transductants exhibited deletions within the 34.8-kb *Bam*HI fragment. In addition, the *Pst*I restriction profile of the plasmids from these transductants showed that no deletions were observed within the 6.3-kb *Pst*I fragment, suggesting that this fragment is located at the end of the large *Bam*HI fragment. By process of elimination, this evidence suggested that the 5.2-kb *Pst*I fragment is located between the 9.3-kb and 6.3-kb *Pst*I fragments. Based on the evidence presented above, the order of the *Pst*I fragments within the 34.8-kb *Bam*HI fragment is shown in Fig. 2.

The results obtained from double digestion and previous restriction analysis of the deletion derivatives from tp21 and tp39 were used to calculate the ends of the deletions within these plasmids. The deletions which were within the toxin-encoding region of the plasmids from these mutants is shown in Fig. 2 by the dotted lines. The *Bam*HI restriction profile of the plasmid from tp21 showed that it was missing the 34.8-kb, 13.9-kb, and 6.0-kb fragments; however, an additional fragment, 44.2 kb in size, was observed (Table 3). DNA-DNA hybridizations of digested pXO1.1 from UM23 with the ^{32}P-labelled 44.2-kb *Bam*HI fragment of the plasmid from tp21 showed that the 44.2-kb fragment hybridized to the 34.8-kb and 13.9-kb *Bam*HI fragment. Results obtained from double digestion of the plasmid from this mutant showed that *Sal*I cut the 44.2-kb fragment into two fragments approx. 36 kb and 8.5 kb in size. The *Pst*I restriction profile of this plasmid showed that it contains intact the 6.3-kb, 5.2-kb, 9.3-kb, and 6.6-kb fragments within the 34.8-kb *Bam*HI fragment. The evidence presented thus far suggested that the 36-kb *Bam*HI-*Sal*I fragment is homologous to the 34.8-kb *Bam*HI fragment and that the 8.5-kb *Bam*HI-*Sal*I fragment is homologous to the 13.9-kb *Bam*HI fragment. By subtracting the size of the *Sal*I arm of Tn*917* from the altered *Bam*HI-*Sal*I fragments, one end of the deletion was calculated to be approx. 6 kb within the 13.9-kb *Bam*HI fragment

and the other end of the deletion was calculated to be approx. 3 kb from the end of the 6.0-kb *Pst*I fragment (Fig. 2).

Similarly, phenotypic characterization of tp39 and restriction analysis of the deletion derivative from tp39 provided evidence that suggested the altered 33-kb and 5.5-kb *Bam*HI-*Sal*I fragments observed from the double digestion of this plasmid with *Bam*HI and *Sal*I were homologous to the 34.8-kb and 7.4-kb *Bam*HI fragments of pXO1.1, respectively. By subtracting the size of the *Sal*I arm of Tn*917* from the altered *Bam*HI-*Sal*I fragments, one end of the deletion was calculated to be approx. 3 kb within the 7.4-kb *Bam*HI fragment and the other end of the deletion was calculated to be approx. 1 kb from the end of the 6.0-kb *Pst*I fragment (Fig. 2). These results suggest that the LF structural gene may be intact in the plasmid from tp39.

Characterization of UM23 tp68. Mutant tp68, which appears to produce PA in the presence and absence of added bicarbonate, was analyzed for PA production in CA broth and CA broth buffered with HEPES (pH 7.5) with or without the addition of sodium bicarbonate. The cultures were incubated at 37°C and 30°C statically or with shaking. The results were inconsistent suggesting that the insertion mutation within the plasmid from tp68 is not stable. The stability of the insertion mutation in tp68 was determined by examining the retention of MLS resistance. Spores of tp68 were streaked onto L agar containing inducing concentrations of erythromycin and grown overnight at 30°C. Individual colonies were picked to L agar and L agar containing inhibitory concentrations of erythromycin and lincomycin. Approximately 10 to 20% of the colonies examined were MLS sensitive. These results suggest that Tn*917*, which appeared to have inserted within the LF structural gene, affected the stability of the plasmid.

Several MLS-sensitive and MLS-resistant derivatives of tp68 were isolated for further examination. Plasmid profiles from these isolates showed that two of the eight MLS^S derivatives were devoid of any plasmids while all of the MLS^r and the other six MLS^S derivatives contained a plasmid which comigrated with wild-type pXO1.1. The plasmids from the tp68 isolates were digested with *Bam*HI to determine whether there were any differences in their restriction patterns. Those from the MLS^r derivatives exhibited *Bam*HI restriction patterns similar to those for pXO1.1::Tn*917* from tp68. The plasmids from the MLS^S derivatives exhibited *Bam*HI restriction patterns similar to those of pXO1.1 from the UM23 parent strain. These results suggested that the loss of MLS^r by a particular population of tp68 can occur by the loss of the Tn*917*-tagged plasmid from the cell or the excision of Tn*917* from the plasmid. Therefore, in order to retain MLS resistance and Tn*917* insertion, tp68 was grown under constant antibiotic selection.

Since tp68 did not grow well on CA-agarose haloimmunoassay plates, growth was examined on L agar, Min IIIB agar (a modified Min IB medium which is a more complete synthetic medium), and Min XO agar (a minimal synthetic medium) at 37°C and 30°C. All media except L agar were supplemented with uracil to satisfy the auxotrophic requirement and with inhibitory concentrations of erythromycin and

lincomycin. Tp68 grew very well on L and Min IIIB agar media both at 37°C and 30°C. While tp68 grew well on Min XO agar at 30°C, it did not grow on that medium at 37°C. These results suggested that tp68 required other nutrients to grow on minimal medium at 37°C and that the Min IIIB agar contained the nutrients necessary to support growth of tp68 at this temperature. tp68 was tested for growth on Min XO agar with paper disks containing each of the nutrients from Min IIIB. Growth was enhanced around the disk containing valine and to a lesser extent around the disk containing leucine. These results suggested that valine and possibly leucine were required for growth at 37°C. This requirement does not appear to be an auxotrophic requirement because valine is not required for growth by the tp68 derivatives cured of pXO1.1::Tn*917* or those in which Tn*917* had excised from the plasmid. This evidence suggested that the Tn*917* insertion within the plasmid from tp68 is responsible for the alteration in ability to grow on minimal medium, a pXO1.1-associated phenotype.

Further analysis of the growth of tp68 in minimal XO broth in the presence or absence of valine showed that although valine enhanced growth of this mutant slightly at 37°C and 30°C, the cells grew poorly in these media. Since tp68 grew better on minimal agar medium supplemented with valine at 37°C, the agar may supply a nutrient necessary to support the growth of tp68. To test this possibility, tp68 was grown on minimal medium containing agarose, a more purified form of agar. The results from these experiments showed that tp68 grew poorly on this medium in the presence or absence of valine at 37°C and 30°C; however, large colony mutants were observed on medium containing valine. These large colony mutants of tp68 no longer require valine for growth. Restriction analysis of the plasmids from these mutants may provide evidence which would explain why these mutants no longer required valine for growth.

UM23 tp68 and its derivatives were examined for alterations in extent of sporulation, a pXO1.1-associated phenotype. The isolates were streaked onto NBY-Mn slants and NBY-Mn slants containing inhibitory concentrations of erythromycin and lincomycin (for tp68 MLS^r derivatives). The slants were incubated at 37°C and 30°C and after 36 and 72 h the isolates were examined for sporulation by phase contrast microscopy. Sporulation of tp68 and its derivatives was compared to the sporulation of UM23 and UM23C1. The results showed that tp68 and its MLS^r derivatives are oligosporogenous (Osp^+) at 30°C and 37°C, whereas, UM23 is Spo^+ at 30°C, Osp^+ at 37°C and UM23C1 is Spo^+ at both temperatures. Like UM23, MLS^s derivatives of tp68 containing pXO1.1 from which Tn*917* had excised were Osp^+ at 37°C and sporulated extensively at 30°C. MLS^s derivatives of tp68 cured of pXO1.1::Tn*917* sporulated extensively at both temperatures which was similar to that observed for UM23C1. These results suggested that Tn*917* insertion within the plasmid from tp68 is responsible for the altered sporulation phenotype.

UM23 tp68 was examined again for PA production in CA broth and CA-HEPES (pH 7.5) broth with and without bicarbonate and with antibiotic selection. The cultures were grown statically at 37°C and

30°C for 30 h and 48 h. As determined from several trials, the results obtained for PA production by tp68 were not reproducible.

Thus, analysis of tp68 showed that it exhibits an alteration in sporulation and in its ability to grow on minimal medium and synthesize PA. As shown in Fig. 2, the location of the Tn*917* insertion in the plasmid from tp68 appears to be within the LF structural gene. This insertion mutation appears to deleterious to the cell and therefore the insertion is unstable. Without antibiotic selection, Tn*917* is excised from the plasmid or cells are cured of the Tn*917*-tagged plasmid derivatives. The next goal in characterizing tp68 would be to isolate and characterize a more stable mutant of tp68.

Optimizing conditions for toxin production by *B. anthracis* Weybridge A UM23 and tp62. As stated above, tp62 produces PA and LF in the absence of added bicarbonate and it overproduces both proteins when bicarbonate is added to the medium. The standard growth conditions used in our laboratory for optimal PA production include growing the strains statically in CA broth with added bicarbonate and charcoal in cotton-plugged flasks. Previous analysis of PA production by UM23 and tp62 grown in several buffered CA media without added bicarbonate statically or with aeration for various times showed that tp62 produced maximum amounts of PA when it was grown in CA broth buffered with 0.05 M HEPES (pH 7.5) with slow shaking (100 rpm) for 15 h.

The optimal conditions for PA production by UM23 and tp62 were determined in CA broth and CA-HEPES broth (pH 7.5) with and without added bicarbonate, heat-inactivated horse serum, and charcoal. The cultures were grown in cotton-plugged flasks with shaking (100 rpm) for 15 h at 37°C. Table 4 lists the conditions tested and the PA titers obtained. Very little PA was produced by either strain in CA broth unless HEPES buffer was added. (In shaken flasks with bicarbonate added the pH probably goes too high). The highest titer produced by UM23 was in CA-HEPES with added bicarbonate and horse serum; the titer was >16<32. UM23 tp62 produced PA at titers of >16<64 in almost all CA-HEPES broths and addition of bicarbonate or charcoal did not seem to affect PA synthesis. However, the addition of horse serum did boost the PA yields somewhat. Horse serum may protect PA from being hydrolyzed by proteases. A dramatic difference between UM23 and UM23 tp62 was observed in CA-HEPES without any additives. The titer with tp62 was 32, whereas no PA was detected in UM23 culture filtrates under these conditions. The results summarized in Table 4 confirm that tp62 does not require added bicarbonate for PA synthesis; they also show that the role played by charcoal in enhancing PA synthesis by UM23 is of no consequence in PA synthesis by tp62.

UM23 and tp62 were then grown in CA-HEPES broth with and without added bicarbonate and horse serum in cotton-plugged and screw-capped flasks with slow shaking to determine whether the environment produced within the flasks under these conditions might affect PA production. A small increase was observed in PA production by both strains when they were grown in the presence of bicarbonate and

horse serum in screw-capped flasks (data not shown). Cultures grown in the presence of bicarbonate in cotton-plugged flasks exhibited a final pH of 8 or greater, whereas those grown under similar conditions in screw-capped flasks exhibited a final pH of 7.1-7.3. In the absence of bicarbonate, no differences in pH and PA production were observed among cultures grown in cotton-plugged and screw-capped flasks. The final pH of these cultures was always below 6.5. Therefore, screw-capped flasks were used in studies testing PA production by insertion mutants grown in the presence or absence of added bicarbonate.

Finally, we wanted to determine the time at which UM23 and tp62 produced maximal amounts of PA, LF, and EF under the conditions described above. To ensure that the broths were inoculated with similar numbers of cells, one-tenth ml of an overnight culture grown in CA broth was transferred to the screw-capped flasks. The cultures were harvested at times ranging from 8 to 25 h. One flask was set up for each time point. At each time interval a 10-ml sample was mixed with 0.5 ml of horse serum, filtered through a Millipore HA membrane, and assayed for PA, LF, and EF. To compare different strains for production of toxin and account for differences in growth, the yields of the toxin components were expressed as μg per ml of cell dry weight. For this the cells were collected on Millipore DA membranes and washed several times with water. The membranes were dried and the dry cell weight was determined.

Tables 5 and 6 show the amounts of PA, LF, and EF produced by UM23 and tp62 grown in the presence and absence of added bicarbonate and horse serum for several time periods. The results show that the time at which UM23 and tp62 produced maximum amounts of the three toxin components in CA-HEPES broth in the presence and absence of added bicarbonate and horse serum was between 12.5 and 15 h. The results in Table 5 also show that when bicarbonate was present in the medium tp62 produced almost twice as much PA and LF as did UM23 under the same conditions. In addition the results in Table 6 confirm that bicarbonate is not necessary for production of PA, LF, and EF by tp62.

Quantitative analysis of toxin production by several insertion mutants. As shown in Table 7, several insertion mutants were examined for production of PA, LF, and EF under conditions described above. The mutants were grown in CA-HEPES broth in the presence and absence of added bicarbonate and horse serum. Insertion mutants tp1A, tp2A, tp20, tp27, tp28, tp36, and tp40 exhibited a toxin phenotype very similar to that of UM23. All except tp27 contain Tn*917* insertions outside of the region of pXO1.1 encoding the toxin genes. Like UM23, most of the insertion mutants except tp62 produced small or no detectable amounts of PA, LF, or EF in the absence of added bicarbonate and horse serum. UM23 tp21, tp39, tp49, and tp71 all contain deletions within pXO1.1 ranging from 16 to 150 kb which presumably were mediated by Tn*917*. All deletants exhibited alterations in production of one or more of the toxin components. DNA-DNA hybridizations of the digested plasmid derivatives from these deletants to the cloned structural genes confirmed some of the toxin phenotypes (discussed below).

UM23 tp21 is deficient in the production of PA because the PA structural gene has been deleted. This mutant does produce more LF and EF in the presence of added bicarbonate than does the UM23 parent strain and only small amounts of these components were produced in the absence of added bicarbonate. The insertion mutant tp72 also exhibited a toxin phenotype similar to that observed for tp21; it produced approx. 20-fold less PA than did UM23. Tn917 in tp72 is inserted within the PA structural gene. In the presence of bicarbonate and horse serum tp72 produced EF and twice as much LF as that observed for UM23 . Small amounts of LF and EF were detected in filtrates of this mutant grown in the absence of bicarbonate and horse serum. The results obtained from analysis of tp21 and tp72 suggest that interruption or deletion of *pag* may affect production of LF and EF.

The deletants, tp49 and tp71, produced reduced amounts of EF and PA, respectively. In addition tp49 produced more PA in the presence of added bicarbonate and horse serum than did the parent strain, and, similarly, tp71 produced five- to six-fold more LF. The resulting toxin phenotype for tp49 is PA^{++}, LF^{+}, and $EF^{+/-}$ and the phenotype for tp71 is $PA^{+/-}$, LF^{++}, and EF^{+}. Results from hybridization of the digested plasmids from these mutants with the cloned toxin structural genes suggest that the phenotypes for tp49 and tp71 should be PA^{+}, LF^{+}, EF^{-}, and PA^{-}, LF^{+}, EF^{-}, respectively. These discrepancies in the toxin phenotypes along with results from restriction analysis of the plasmids from these strains suggested that the spore stocks of each mutant may contain a mixed population of deletants. This has been confirmed and we are now in the process of attempting to segregate the appropriate deletants by phage CP-51-mediated transduction.

The insertion mutants tp29 and tp32 and the deletant tp39 are deficient in production of all three toxin components. The difference between these mutants is that pXO1.1 in tp29 and tp32 contains an insertion mutation within the gene encoding the positive trans-acting factor (discussed below) and the plasmid in tp39 contains a 30-kb deletion encompassing *pag*, *cya*, and the positive trans-acting factor.

Analysis of the filtrates from tp62 confirmed that it produces more PA and LF in the presence of added bicarbonate and horse serum than does the parent strain. In addition, tp62 produced approx. 25-fold more PA in the absence of added bicarbonate and horse serum than that observed for UM23. Thus, although bicarbonate is not necessary for production of the three toxin components by tp62, increased yields of all three were observed when bicarbonate and horse serum were added to the medium. The PA observed from filtrates obtained from tp62 grown in the absence of added bicarbonate may be proteolytically degraded. Experiments are being conducted to determine whether PA, LF, and EF might be more stable in filtrates obtained from tp62 grown in the absence of added bicarbonate and horse serum if the culture is neutralized to reduce protease activity.

Analysis of the toxin phenotypes of UM23 tp62 and tp29. The mutant toxin plasmids from tp62 and tp29 were moved individually by conjugation into UM23C1-2, a rifampicin-resistant mutant of

UM23C1(pXO1.1)$^-$. This was done by first introducing pBC16 and the conjugative plasmid pXO12 carrying Tn*917* (pXO12::Tn*917*) into tp62 and tp29 by mating (1). Transcipients from these matings were than used as donors to transfer pXO1.1::Tn917 to UM23C1-2 and selecting transcipients that were Rif^r and MLS^r.

Four transcipients, designated UM23C1-2 tr1-62 to tr4-62, were isolated from the mating with tp62 as the donor and four, designated UM23C1-2 tr1-29 to tr3-29, were isolated from the mating with tp29 as the donor. Plasmid profiles showed that the transcipients had acquired a plasmid which comigrated with pXO1.1::Tn*917* from tp62 or pXO1::Tn*917* from tp29, respectively. The transcipients tested positive when screened for PA production in CA broth and on CA-agarose haloimmunoassay plates. *B. thuringiensis* crystals, the synthesis of which is encoded by pXO12, were produced when these transcipients sporulated indicating that pXO1.1 and pXO12 probably exist as cointegrates or recombinants. Results in Table 8 show that the transcipients resembled their respective donor parent with respect to PA production.

Tp62 also exhibited alterations in the extent of sporulation, a pXO1.1-associated phenotype. It is Osp$^+$ at 30^{o}C and 37^{o}C, whereas the parent strain Weybridge A UM23 is Spo$^+$ at 30^{o}C and Osp$^+$ at 37^{o}C. The transcipients carrying pXO1::Tn*917* from tp62 exhibited the same sporulation phenotype as that observed for tp62. These results suggested that the Tn*917* insertion in pXO1.1 may also be responsible for the altered sporulation phenotype. To confirm this tp62 was cured of pXO1.1::Tn*917* by serial transfers at 43^{o}C. The cured strains were MLS^s, indicating that in tp62 Tn*917* was inserted only in the plasmid, and their sporulation phenotype was the same as that of UM23 cured of pXO1.1, i.e., they were Spo$^+$ at 30^{o}C and 37^{o}C. These results provide further evidence that the Tn*917* insertion in pXO1.1 of tp62 is responsible for the altered sporulation phenotype.

Identification of a gene on pXO1.1 involved in positive activation of toxin synthesis. As shown above, insertion mutants Weybridge A UM23 tp29 and tp32 are deficient in production of all three components of the anthrax toxin. The location of Tn*917* in pXO1.1 from tp29 and tp32 is between the PA and EF structural genes and within 2 kb of the end of a 13.9-kb *Bam*HI fragment. This suggested that this region of pXO1.1 may be involved in positive regulation of toxin production. We were unsuccessful in cloning the 13.9-kb *Bam*HI fragment. We were successful, however, in cloning into a gram-negative vector an 8.0-kb *Eco*RI fragment that overlaps the 13.9-kb *Bam*HI fragment and encompasses the positive regulatory region. The clone was designated *E. coli* DH5α etf2-8.0.

While we were involved in the cloning project, I. Uchida, working in Dr. S. Leppla's laboratory at NIDR in Bethesda, MD, and taking advantage of information presented by Hornung and Thorne at the 1991 ASM meeting (4), was successful in cloning this positive regulatory region in pHY300PLK and sequencing the cloned fragment. Two open reading frames were identified, but only one appears to be involved in positive regulation of toxin synthesis. Because this work was initiated in my laboratory and was made possible by Jan Hornung's isolation and characterization of insertion mutants tp29 and tp32, it seemed

logical that the two laboratories should collaborate in completion of the project. Jan Hornung has spent some time in Dr. Leppla's laboratory making certain that the gene cloned in his laboratory is the same gene that she cloned, i.e., the gene of interest to us. The restriction pattern of the 8.0-kb insert in the recombinant plasmid from *E. coli* DH5α etf2-8.0 was compared with that of the cloned insert that I. Uchida obtained. Uchida's cloned insert contains a 3.5-kb *Bam*HI-*Eco*RI fragment similar to that observed for the 8.0-kb *Eco*RI insert. In addition, I. Uchida subcloned the major ORF and he and Hornung showed that it complemented the insertion mutation within tp29 and tp32. Furthermore, PCR analysis carried out by Uchida showed that the insertion mutations in the plasmids derived from tp29 and tp32 were located within the major ORF involved in activation of toxin synthesis. These results suggest that the DNA cloned by Uchida, as well as that cloned by Jan Hornung, contains the gene involved in positive regulation of synthesis of the toxin components. The gene has been given the designation *atxA*, and a manuscript describing the cloning and characterization of the gene is in preparation (23).

Cloning of a region of pXO1.1 involved in negative regulation of toxin synthesis. As discussed above and shown in Table 7, tp62 does not require added bicarbonate for synthesis of toxin. Tn*917* in pXO1.1 from tp62 is located on a 9.3-kb *Pst*I fragment just upstream of the LF structural gene (Fig. 2), suggesting that this region may be involved in negative regulation of toxin synthesis. The *Pst*I restriction profile of pXO1.1 showed that there are two 9.3-kb fragments. To clone the region involved in negative regulation, the 9.3-kb *Pst*I fragment containing the putative negative regulator gene was isolated from pXO1.1::Tn*917* of tp28 which contains an insertion in the other 9.3-kb fragment. The fragment was then cloned into pBluescriptIIKS+ and the ligation mixture was transformed into *E. coli* DH5α by electroporation. One transformant was isolated that contained a recombinant plasmid with a 9.3-kb *Pst*I insert and was designated *E. coli* DH5α etf2-9.3. DNA-DNA hybridization of the digested recombinant plasmid from etf2-9.3 with the 8.6-kb *Pst*I fragment of pXO1 from *B. anthracis* Sterne (USAMRIID) showed that the 8.6-kb fragment hybridized to the cloned insert. As discussed below, the 8.6-kb *Pst*I fragment of pXO1 from Sterne (USAMRIID) shares homology with the 9.3-kb *Pst*I fragment of pXO1.1 from Weybridge A UM23 (Fig. 6). In addition, the *Eco*RI restriction profile of the 14.7-kb *Pst*I fragment, i.e., the altered 9.3-kb *Pst*I fragment of pXO1.1::Tn*917* from tp62 that contains Tn*917*, was similar to that observed for the 9.3-kb *Pst*I insert of the recombinant plasmid from etf2-9.3. The only difference observed in the restriction profiles was that the 14.7-kb *Pst*I fragment was missing a 1.2-kb *Eco*RI fragment and contained an additional fragment approx. 6.7 kb in size. The 6.7-kb *Eco*RI fragment corresponded to the insertion of Tn*917* in the 1.2-kb *Eco*RI fragment. These results suggested that we had cloned the 9.3-kb *Pst*I fragment of interest. We now hope to subclone a smaller fragment of the 9.3-kb *pst*I insert encompassing the putative negative regulatory gene into a Gram-positive cloning vector, pHPS9, and transform the ligation mixture into *B.*

subtilis 6GM15 by protoplast transformation. The cloning and characterization of the negative regulatory region has become a collaborative project with I. Uchida and S. Leppla at NIDR in Bethesda, MD.

DNA-DNA hybridization analysis of pXO1.1::Tn*917* deletion derivatives with cloned toxin structural genes. The pXO1.1::Tn*917* deletion derivatives from tp21, tp39, tp49, and tp71 were tested for hybridization to the cloned LF and EF structural genes to determine what toxin genes were present. Plasmids pLF7 and pSE42 containing cloned LF and EF structural genes, respectively, were digested with either *Eco*RI or *Bam*HI. The 7.4-kb *Bam*HI fragment from pSE42 and all *Eco*RI fragments pooled from pLF7 were labelled with digoxigenin-dUTP and used to probe *Pst*I- and *Bam*HI-digested plasmids from deletion derivatives. The results are shown in Table 9.

All of the deletion derivatives examined contain the LF structural gene and all but tp39 produce LF (Table 7). The results obtained from restriction analysis of the plasmid from tp39 showed that the deletion within this plasmid encompasses the positive activating factor gene atxA. Thus, no LF is detected in filtrates from tp39 because the LF gene is not being expressed. As discussed below, when the recombinant plasmid containing the cloned *atxA* gene was transformed into tp39, production of LF was detected.

Plasmids from tp21 and tp39 hybridized to the EF gene probe, but as shown in Table 7, only tp21 produces EF. As discussed above, results obtained from restriction analysis determining the ends of the deletion within the plasmid from tp39 suggested that the EF structural gene on the 7.4-kb *Bam*HI fragment had been deleted; however, 3 kb of this fragment was still present. Since the 7.4-kb *Bam*HI fragment containing the EF gene was cloned in its entirety, this explains why it should hybridize to the partially deleted 7.4-kb *Bam*HI fragment of the plasmid from tp39.

The EF probe did not hybridize to the 40-kb plasmid from tp49 or to the 47.5-kb plasmid from tp71. However, it did hybridize to fragments of the digested plasmids from tp49 and tp71 that were only weakly visible on the stained gel and which were shown to comigrat with digested fragments from pXO1.1. As discussed above, these results suggested that the spore stocks of tp49 and tp71 contain a mixed population of deletants. DNA-DNA hybridization analysis of the plasmids from these mutants will be reexamined once we have succeeded in segregating the 40-kb deletion derivative of tp49 and the 47.5-kb deletion derivative of tp71.

Previous restriction analysis and hybridization analysis of the deletion derivatives from tp21, tp39, tp49, and tp71 showed that only the plasmid from tp49 should contain a PA structural gene (5,7). The data presented in Table 7 show that only tp49 produces large amounts of PA.

Introduction of pIU51 into UM23 tp39. Restriction analysis of the plasmid from tp39 suggested that an intact LF gene is present. However, since the deletion within this plasmid encompasses the positive activating factor gene, no LF production detected. Introduction of the cloned positive activating

factor gene into this strain should allow expression of the LF gene if it is intact. If the LF gene can be expressed in this manner, then the mutant should be able to produce LF uncontaminated with PA or EF.

The tetracycline-resistance recombinant plasmid, pIU51, which contains the cloned positive activating factor gene, was introduced into tp39 by electroporation. Transformants tp39 etf3 and etf5 were analyzed for production of PA, LF, and EF. Plasmid pIU51 did not appear to be maintained stably in the tp39 transformants unless they were grown under selection with tetracycline. When tp39 etf3 and etf5 were grown in CA-HEPES (pH 7.5) in the presence of bicarbonate, horse serum and inhibitory concentrations of tetracycline, only LF was produced. The concentration of LF appeared to be about ten-fold lower than that observed for UM23. No detectable amounts of PA or EF were present within the filtrates. We would like to optimize growth conditions for these transformants to determine whether the amount of LF produced by these tp39 transformants can be increased.

II. Analysis of an inversion encompassing the toxin-encoding region of pXO1.1 (Weybridge A) and pXO1 (Sterne).

Identification of an inversion. The *Bam*HI and *Pst*I restriction profiles of pXO1.1 from *B. anthracis* Weybridge A UM23 as determined in our laboratory differed from those published by Robertson et *al.*(10) for pXO1 from a different pXO1^{+}, pXO2^{-} strain (labeled Sterne). The difference was observed in the region surrounding the toxin structural genes (4). As shown in Fig. 4, the 29-kb and 19-kb *Bam*HI fragments shown on the restriction map of pXO1 constructed by Robertson *et al.* differed from the 34.8-kb and 14.6-kb fragments generated by *Bam*HI digestion of pXO1.1. The restriction map of pXO1.1 shown in Fig. 5 is based on the map of pXO1 constructed by Robertson *et al.* and results obtained from restriction analysis of pXO1.1, pXO1.1::Tn*917* derivatives, and deletion derivatives and DNA-DNA hybridizations of digested pXO1.1 with the cloned toxin structural genes.

Double digestion of pXO1.1 with *Bam*HI and *Sal*I showed a restriction profile which differed from that deduced from Robertson's map. Three *Sal*I restriction sites were observed in pXO1.1. They are located in the 38.7-kb 19.9-kb and 14.6-kb *Bam*HI fragments and corresponded to those in the 37-kb, 20-kb, and 29-kb *Bam*HI fragments on Robertson's map, respectively. These results suggested that the 14.6-kb fragment of pXO1.1 was homologous to the 29-kb fragment of pXO1 (Robertson).

In addition to the differences observed for the *Bam*HI restriction profiles, *Pst*I digestion of pXO1.1 generated an 18.7-kb and a 9.3-kb fragment instead of a 20-kb and an 8.6-kb fragment depicted on Robertson's map. The differences in *Pst*I restriction patterns can be seen in Fig. 5. Results from homologous DNA-DNA hybridizations showed that the 9.3-kb as well as the 6.6-kb, 6.3-kb, 6.0-kb, and 5.2-kb *Pst*I fragments from pXO1.1 were nested within the 34.8-kb *Bam*HI fragment. DNA-DNA hybridization

studies using the cloned toxin structural genes as well as secondary digestion of the 34.8-kb fragment provided evidence that the *Pst*I fragments homologous with the *Bam*HI fragment are the five fragments listed above. DNA-DNA hybridizations of digested pXO1.1 with the cloned LF structural gene showed that it hybridized to the 34.8-kb *Bam*HI fragment and to the 6.6-kb and 6.0-kb *Pst*I fragments. According to Robertson's map *lef* is located on the 6.6-kb and 6.0-kb *Pst*I fragments which are nested within the 29-kb *Bam*HI fragment. Robertson's map also shows that the 19-kb *Bam*HI fragment contains *Pst*I fragments which may correspond to the 9.3-kb, 6.3-kb, and 5.2-kb *Pst*I fragments located within the 34.8-kb *Bam*HI fragment of pXO1.1. These results suggested that the 34.8-kb *Bam*HI of pXO1.1 shares homology with the 29-kb and 19-kb *Bam*HI fragments of pXO1 from Robertson's strain.

The evidence presented above suggested that the region encompassing the toxin structural genes in pXO1.1 from Weybridge A UM23 may be inverted in comparison to the toxin-encoding region shown on the restriction map of pXO1 constructed by Robertson *et al.* The orientation of the region encoding the toxin structural genes has been designated as α for pXO1 from Robertson's *B. anthracis* strain and as ß for pXO1.1 from Weybridge A UM23 (19).

The restriction profiles for pXO1 isolated from other *B. anthracis* ($pXO1^+$, $pXO2^-$) strains, including Weybridge, Weybridge A, Weybridge B, Sterne (USAMRIID), Anvax, V770, PM36R-1, Ames ANR-1, and New Hampshire NNR-1, were examined (4). All except Sterne (USAMRIID) exhibited restriction profiles similar to the profiles exhibited by pXO1.1 from Weybridge A UM23 and therefore, all most likely carry the toxin-encoding region in the ß orientation. The toxin plasmid from Sterne (USAMRIID) generated *Bam*HI, *Bam*HI-*Sal*I, and *Pst*I restriction patterns which corresponded to those shown for pXO1 by Robertson. Thus the toxin-encoding region of pXO1 from Sterne (USAMRIID) is most likely in the α orientation. The origin of the Sterne strain used by Robertson *et al.* (10) has not been determined; however, it seems likely this the strain he used is the same as the Sterne (USAMRIID) strain.

Physical mapping of the toxin-encoding region of pXO1.1 from *B. anthracis* Weybridge A UM23 and pXO1 from Sterne (USAMRIID). As shown in Fig. 5, a *Bam*HI, *Bam*HI-*Sal*I, and *Pst*I restriction map was constructed for a 77-kb region of pXO1.1 encompassing the toxin structural genes. Results from restriction analysis with single, double, and triple digestions of pXO1.1, pXO1.1::Tn*917*, and deletion derivatives were used to construct this restriction map. DNA-DNA hybridizations of digested pXO1.1 with the cloned toxin structural genes and localization of Tn*917* in pXO1.1 from UM23 tp2A, tp29, tp32, tp36, and tp62 (discussed above) also provided evidence to delineate the positions of the restriction fragments within the toxin-encoding region. The map of the toxin-encoding region of pXO1 from Sterne (USAMRIID) was constructed based on the map of pXO1 constructed by Robertson, *et al.* (10), restriction analysis of the plasmid, and DNA-DNA hybridizations of the digested plasmid with the cloned toxin structural genes.

Digestions of the larger *Bam*HI and *Pst*I fragments found within the toxin-encoding region of pXO1.1. Table 10 shows results of the digestion of the 34.8-kb *Bam*HI fragment with *Pst*I and the 18.7-kb and 18.1-kb *Pst*I fragments with *Bam*HI. Restriction analysis of the 34.8-kb *Bam*HI fragment with *Pst*I confirmed that the 9.3-kb, 6.6-kb, 6.3-kb, and 5.2-kb *Pst*I fragments were nested within this *Bam*HI fragment. A 4.7-kb fragment that comigrated with a *Pst*I fragment from pXO1.1 was also shown to be part of the 34.8-kb *Bam*HI fragment. As discussed previously, this large *Bam*HI fragment hybridized to a 6.0-kb *Pst*I fragment rather than to a 4.7-kb fragment. The location of *pag* and *lef* is in part within the 6.0-kb *Pst*I fragment; however, both genes are located on different *Bam*HI fragments. This observation suggested that the 6.0-kb *Pst*I fragment contains a *Bam*HI site. The sequence of *pag* (24) showed that a *Pst*I restriction site is located approx. 1.4 kb from a *Bam*HI restriction site. This value corresponded to the difference between the 6.0-kb *Pst*I fragment which hybridized to the 34.8-kb *Bam*HI fragment and the 4.7-kb fragment resulting from the digestion of the *Bam*HI fragment. Thus, this evidence suggested that the 4.7-kb fragment of the 34.8-kb *Bam*HI fragment is homologous to the 6.0-kb *Pst*I fragment of pXO1.1. The order of the *Pst*I fragments within this large *Bam*HI fragment was determined from data obtained from DNA-DNA hybridization of digested pXO1.1. with recombinant plasmids containing the cloned *pag* or *lef* gene, the location of Tn*917* in pXO1.1 derivatives from tp2A, tp36, and tp62 (discussed above), and previous restriction analysis of the deletion derivatives of UM23C1 tds1, tds2, and tds6. The order of the *Pst*I fragments within the 34.8-kb *Bam*HI fragment is shown in Figs. 2 and 5.

The *Bam*HI restriction profile of the 18.7-kb *Pst*I fragment showed that it contains a 14.6-kb fragment that comigrates with the 14.6-kb *Bam*HI fragment of pXO1.1. A 2.0-kb and a 2.7-kb fragment were also present, but the location of these fragments has not been determined. The cloned 7.4-kb *Bam*HI fragment of pXO1 containing *cya* has been shown previously to hybridize to the 18.7-kb and 5.5-kb *Pst*I fragments of pXO1. Based on this evidence the 2.0-kb fragment is most likely nested within the 7.4-kb *Bam*HI fragment. By the process of elimination, the 2.7-kb fragment is most likely nested within the 7.7-kb *Bam*HI fragment that is adjacent to the 14.6-kb *Bam*HI fragment (Fig. 5).

When the 18.1-kb *Pst*I fragment of pXO1.1 was digested with *Bam*HI, it was shown to contain a 13.9-kb fragment that comigrated with the 13.9-kb *Bam*HI fragment of pXO1.1 and a 4.8-kb fragment. The cloned 6.0-kb *Bam*HI fragment of pXO1 that contains *pag* has been shown to hybridize to the 6.0-kb and 18.1-kb *Pst*I fragments. Thus, the 4.8-kb *Pst*I-*Bam*HI fragment most likely is homologous to one end of the 6.0-kb *Bam*HI fragment.

Location of the toxin structural genes on pXO1.1 from Weybridge A UM23 and pXO1 from Sterne (USAMRIID). The results of DNA-DNA hybridizations of the *Bam*HI- and *Pst*I-digested plasmids from Weybridge A UM23 and Sterne (USAMRIID) with the cloned PA, LF, and EF structural genes were used to confirm the locations of the toxin genes on pXO1.1 (Weybridge A) and to determine their location

on pXO1 from Sterne (USAMRIID). The plasmids pPA102, pLF7, and pSE42 containing cloned PA, LF, and EF structural genes, respectively, were digested with either *Eco*RI or *Bam*HI. The 7.5-kb *Bam*HI fragment from pSE42, all *Eco*RI fragments pooled from pLF7, and the 2.2-kb *Eco*RI fragment from pPA102 were labelled with digoxigenin-dUTP, and hybridized to *Pst*I- and *Bam*HI-digested plasmids from Weybridge A UM23 or Sterne (USAMRIID). The results are shown in Table 11. The locations of *pag*, *lef*, and *cya* on pXO1.1 (Weybridge A UM23) and pXO1 (Sterne) are depicted in Fig. 5.

The PA structural gene hybridized to a 6.0-kb *Bam*HI fragment and a 6.0-kb *Pst*I fragment of both pXO1 (Sterne) and pXO1.1 (Weybridge A). The LF structural gene hybridized to the same *Pst*I fragments of pXO1 from both strains, but to different *Bam*HI fragments. The EF probe hybridized to the same *Bam*HI fragment, however, a difference was observed upon hybridization to the *Pst*I fragments. The EF probe hybridized to the same 5.5-kb *Pst*I fragment, but it hybridized to an 8.6-kb *Pst*I fragment of pXO1 (Sterne) and to an 18.7-kb *Pst*I fragment of pXO1.1 (Weybridge A). These results provided more evidence that an inversion had occurred in one of the plasmids.

Digestion of pXO1.1 (Weybridge A) and pXO1 (Sterne) with *Bam*HI and *Sal*I. The *Bam*HI and *Bam*HI-*Sal*I restriction profiles for pXO1.1 (Weybridge A UM23) and pXO1 (Sterne) are shown in Table 12. As predicted from Robertson's restriction map of pXO1, three *Sal*I restriction sites were found in the plasmids from Weybridge A UM23 and Sterne (USAMRIID). They are located in the 38.7-kb, 19.9-kb, and 14.6-kb *Bam*HI fragments of pXO1.1 (Weybridge A UM23) and the 38.7-kb, 29-kb, and 19.9-kb *Bam*HI fragments of pXO1 (Sterne).

For pXO1.1 (Weybridge A UM23), *Sal*I cuts the 38.7-kb *Bam*HI fragment into two fragments that are 32 kb and 6.7 kb in size. This result was confirmed by double digestion of two Tn*917*-tagged deletion derivatives of pXO1.1::Tn*917* from UM23 tp1A (UM23C1 tds4d and tds9). The location of Tn*917* in pXO1.1 from UM23 tp1A is in the 38.7-kb *Bam*HI fragment creating a fragment approx. 46 kb in size. The altered 38.7-kb *Bam*HI fragment remained intact within the deletion derivatives from UM23C1 tds4d and tds9. As discussed previously, Tn*917* contains one *Sal*I restriction site that is located almost in the middle of the transposon. Double digestion of the deletion derivatives from tds4d and tds9 showed that the altered 38.7-kb *Bam*HI fragment is cut by *Sal*I into three fragments, 32 kb, 6.9 kb, and 5.2 kb in size, with the 6.7-kb *Bam*HI-*Sal*I fragment missing (data not shown). These results showed that Tn*917* is located within the 6.7-kb *Bam*HI-*Sal*I fragment and that the 38.7-kb *Bam*HI fragment contains the 32-kb and 6.7-kb *Bam*HI-*Sal*I fragments. Thus the 19.9-kb fragment must be cleaved by *Sal*I producing the 13.9-kb and 6.0-kb *Bam*HI-*Sal*I fragments and the 14.6-kb must be cut by *Sal*I generating the 11.5-kb and 2.8-kb *Bam*HI-*Sal*I fragments.

The *Bam*HI-*Sal*I restriction profile for pXO1 (Sterne) differed from that observed for pXO1.1 (Weybridge A UM23). As predicted from Fig. 4, the *Bam*HI restriction pattern of pXO1 (Sterne) is missing

the 34.8-kb and 14.6-kb *Bam*HI fragments but it contains a 29-kb and 19.5-kb *Bam*HI fragment. The fragments generated by *Sal*I digestion of the 38.7-kb and 19.9-kb *Bam*HI fragments were similar in size to those generated for the same fragments from pXO1.1 (Weybridge A UM23). The 29-kb *Bam*HI fragment was cut by *Sal*I into two fragments, 26.2-kb and 2.8-kb in size. This 2.8-kb *Bam*HI-*Sal*I fragment comigrates with that generated from digestion of the 14.6-kb *Bam*HI fragment of pXO1.1 (Weybridge A UM23). These results supported the evidence suggesting that the 14.6-kb *Bam*HI fragment of pXO1.1 (Weybridge A UM23) is homologous to the 29-kb *Bam*HI fragment of pXO1 (Sterne).

DNA-DNA hybridization analysis of the end restriction fragments of the inverted region of pXO1.1 (Weybridge A UM23) and pXO1 (Sterne). To provide evidence that an inversion had occurred within the toxin-encoding region, restriction fragments encompassing the ends of the inverted segment (shown in Fig. 5 with diagonal lines) were used in DNA-DNA hybridizations to probe the *Bam*HI- and *Pst*I-digested plasmids from Sterne (USAMRIID) and from Weybridge A UM23. The 34.8-kb and 14.6-kb *Bam*HI fragments of pXO1.1 (Weybridge A UM23) and the 19-kb and 8.6-kb *Pst*I fragments of pXO1 (Sterne) were electroeluted and labelled by random priming with digoxigenin-labelled dUTP. The results of these experiments are shown in Table 13 and the probable ends of the inversion are depicted in Fig. 5. As predicted above, the 34.8-kb and the 14.6-kb *Bam*HI fragments of pXO1.1 (Weybridge A UM23) share homology with the 29-kb *Bam*HI fragment of pXO1 (Sterne). The 34.8-kb *Bam*HI fragment also shares homology with the 19.5-kb *Bam*HI fragment of pXO1 (Sterne). Similarly, the 19-kb and the 8.6-kb *Pst*I fragments of pXO1 (Sterne) share homology with the 18.7-kb and the 9.3-kb *Pst*I fragments of pXO1.1 (Weybridge A UM23). The results of this hybridization analysis confirm that an inversion involving a segment of pXO1 as large as 40 kb has occurred (Fig. 5). To determine whether inverted repeats or insertion sequences were responsible for the inversion, the ends of the inverted segments from pXO1.1 (Weybridge A) and pXO1 (Sterne) will be cloned and sequenced.

Phenotypic characterization of Sterne (USAMRIID) and Weybridge derivatives. As described previously, Weybridge A exhibited differences in pXO1-associated phenotypes from those observed for Weybridge UM44. The Weybridge A strain was isolated from the Weybridge strain as a result of its ability to grow better on minimal medium, a phenotype that was later found to be associated with the presence of pXO1 (11, 16). Other differences in plasmid-associated phenotypes include extent and rate of sporulation and sensitivity to bacteriophages. For these reasons the plasmid from Weybridge UM44-1 has been designated as pXO1 and that from Weybridge A as pXO1.1.

Table 14 lists the plasmid-associated phenotypes tested for *B. anthracis* Weybridge derivatives and Sterne (USAMRIID). Sterne (USAMRIID) exhibited phenotypes similar to those observed for Weybridge, Weybridge UM44-1, and Weybridge B. These strains sporulated extensively at 37^{O}C, grew poorly on minimal medium, were sensitive to the bacteriophage CP-51, and produced about the same amounts of

PA. With the exception of the amount of PA produced by these strains, Weybridge A UM23 exhibited different phenotypes. Weybridge A UM23 was oligosporogenous at 37°C, grew well on minimal medium, and was altered in its sensitivity to CP-51. The plasmids from Weybridge, Weybridge UM44-1, and Weybridge B like that from Weybridge A UM23 carry the toxin-encoding region in the β orientation; whereas, the plasmid from Sterne (USAMRIID) carries this region in the α orientation. Based on these results no phenotypic differences could be attributed to the inversion thus far.

III. Physical and genetic analysis of the *B. anthracis* capsule plasmid pXO2

Until recently *B. anthracis* strains harboring pXO2 could be divided into three groups with respect to capsule phenotype; (i) strains that produce capsule only when grown on media containing bicarbonate and incubated in a CO_2-rich atmosphere (Cap^{c+}, wild-type phenotype); (ii) mutants that produce capsule when grown in air in the absence of bicarbonate (Cap^{a+} phenotype); and (iii) mutants that are noncapsulated under all growth conditions yet retain pXO2 (Cap^- phenotype). Utilization of the temperature-sensitive transposition selection vector pTV1 has allowed the isolation of a collection of pXO2::Tn*917* derivatives. In addition to the mutant phenotypes described above, insertion mutants exhibit the following phenotypes: (i) Mutants that produce greater amounts of capsular material than wild type in the presence of bicarbonate and CO_2; (ii) Mutants that are CO_2-independent for capsule synthesis and whose growth is inhibited by bicarbonate; (iii) Mutants that are Cap^+ when grown in air, and whose growth is inhibited by CO_2; (iv) Mutants that require CO_2 for growth and are Cap^+ in the presence of CO_2 and bicarbonate.

Although pXO2 has been demonstrated to be involved in capsule synthesis by *B. anthracis* (2) and although some, if not all, of the structural genes have been cloned (7), little is known regarding possible regulatory genes which may be present on the plasmid. The phenotype of some insertion mutants suggest that Tn*917* may be inserted in sequences involved in bicarbonate regulation of capsule synthesis. Restriction and DNA-DNA hybridization analysis have shown that in 18 out of 20 insertion mutants examined so far, Tn*917* has inserted in regions outside of the *cap* structural genes reported by Makino, et al. (7). These findings suggest that the insertions may be interrupting regulatory functions.

Efforts in my laboratory have been concentrated on characterization of insertion mutants and location of the *cap* structural genes on pXO2. Restriction analysis with different enzymes has been conducted to narrow the location of the putative regulatory regions and they have revealed two regions that may contain sequences responsible for regulation of capsule synthesis. Experiments are in progress to clone these two regions.

Restriction analysis of the Tn*917*-tagged pXO2 derivatives from *B. anthracis* 4229 UM12. To locate the insertions in the pXO2::Tn*917* derivative restriction analysis with several restriction endonucleases have been performed. Results show that Tn*917* inserted into a number of different sites in pXO2. The locations of Tn*917* were confirmed in all cases by DNA-DNA hybridizations using digoxigenin-labelled Tn*917* as a probe. Results obtained from *Eco*R1 digestions, *Hin*dIII digestions, and *Cla*I digestions are shown in Tables 15, 16, and 17, respectively. Several of the insertion mutants show phenotypic alterations and the phenotypes of some of them suggest that Tn*917* is inserted in sequences involved in regulation of capsule synthesis. Examples of some of these mutants that carry insertions in presumed regulatory genes are tp49 and tp60 which seem to be polypeptide overproducers in the presence of CO_2 and bicarbonate; tp24, a Cap^{a+} strain, which produces capsule in the absence of added bicarbonate and CO_2; and tp21 which is Cap^- under all growth conditions. Each of these has Tn*917* inserted in (i) a 6.3-kb *Eco*RI fragment that migrates in electrophoretic gets as part of a doublet; (ii) a 13-kb *Hin*dIII fragment; and (iii) a 10.5-kb *Cla*I fragment. However, not all insertions within these regions affected capsule production (e.g., tp3 and tp4). As shown in Tables 15, 16, and 17, the tagged plasmids from tp6 and tp38 are missing more than one fragment. The resulting Cap^- phenotype of these transposants may be caused by deletion of these fragments.

***Eco*RI restriction analysis.** All of the mutants described immediately above are missing one of the 6.3-kb *Eco*RI fragments. Insertion of Tn*917* into a 6.3-kb fragment should produce a new fragment approximately 11.9 kb in size (6.3 kb + 5.6 kb from Tn*917*). However, in all instances, except for tp24 and tp21, the new fragment was smaller than expected, suggesting that deletions which are probably mediated by Tn*917* must have occurred. Tn*917* insertion in tp7 has been located within a 2.2-kb *Eco*RI fragment that is also part of a doublet.

***Hin*dIII restriction analysis.** *Hin*dIII cleaves Tn*917* into three fragments approximately 3.0 kb, 1.3 kb, and 1.3 kb in size. The 3.0-kb fragment represents one end of the transposon which encodes the *erm* gene and one of the 1.3-kb fragments represents the other end of the transposon. The remaining 1.3-kb fragment represents the Tn*917* internal fragment. As a result the Tn*917* probe should be expected to hybridize to three new fragments in *Hin*dIII-digested plasmids from insertion mutants. These results are shown in Table 16. Mutants with altered phenotype with respect to capsule production showed insertion of Tn*917* within the largest *Hin*dIII fragment. Two of the insertion mutants are polypeptide overproducers, two are CO_2-independent for capsule synthesis and one is unable to synthesize. However, not all insertions within this region affected capsule production, e.g., tp3 and tp4.

***Cla*I restriction analysis.** *Cla*I cleaves Tn*917* into 6 fragments approximately 2.1 kb, 1.5 kb, 1.1 kb, 0.5 kb, 0.3 kb, and 0.1 kb in size. The 0.3-kb and 0.1-kb fragments represent the ends of the transposon, the remaining fragments represent the Tn*917* internal fragments. Although the Tn*917* probe should be

expected to hybridize to 6 new fragments from *Cla*I-digested plasmids from insertion mutants, only three fragments show hybridization. The amounts of Tn*917* in the smallest internal fragment and the *two* end fragments are too small to be detected by the Tn*917* probe. The altered fragments, the new fragments from *Cla*I-digested plasmids from insertion mutants and the fragments that hybridize to the Tn*917* probe are shown in Table 17.

These analyses of pXO2 from the insertion mutants have made it possible to locate more precisely the Tn*917* insertions on the pXO2 restriction map reported by Robertson (10). Based on this map as a reference, the location of Tn*917* insertions appeared in 18 out of 20 mutants examined thus far to have interrupted regions on pXO2 which are external to the *cap* structural genes. We have suggested previously that a region may exist in the 6.3-kb *Eco*R1 fragment (that is part of a doublet) which plays a role in regulation of capsule synthesis. The 6.3-kb *Eco*R1 fragment has been shown to be nested within the 13-kb *Hin*dIII fragment and to be part of the 10.5-kb *Cla*I fragment, narrowing the location of the putative regulatory region. These restriction analyses have revealed also that the 2.8-kb *Hin*dIII fragment may contain another region involved in regulation of capsule synthesis. The locations of Tn*917* insertion in several mutants are shown in Fig. 6.

To study the regions of pXO2, which appear to be involved in regulation of capsule synthesis, it would be advantageous to clone the fragments into a small multicopy vector. One option, which has been successful for cloning restriction fragments from pXO1, would be to clone in *E. coli* DH5α using the pBluescriptIIKS+ cloning vector. Experiments are in progress to clone these putative regulatory regions. If we are successful in cloning these regions, we will use the clones in complementation experiments to determine whether the cloned genes are involved in regulation of capsule synthesis.

Location of *cap* structural genes on pXO2. The cloned *cap* structural genes were isolated from pUBCAP1 (obtained from I. Uchida) and used in DNA-DNA hybridization experiments to locate the *cap* genes on pXO2 from *B. anthracis* 4229 UM12, 6602 and several 4229 UM12 insertion mutants. The cloned structural genes represent the 3.8-kb and 2.5-kb *Xba*I fragments of pXO2 from strain Davis TE702 and correspond to the G and J fragments, respectively, on the pTE702 restriction map constructed by Uchida, et al. (22). The cloned fragments from pUBCAP1 were isolated from gels by electroelution, labeled with digoxigenin-labeled dUTP and used as probes in DNA-DNA hybridization experiments.

In summary, the 2.5-kb *Xba*I fragment (J fragment) hybridized to the following fragments of pXO2 from wild-type strains TE702, 4229 UM12, and 6602; (i) 2.5-kb *Xba*I fragment, (ii)6.6-kb, 4.2-kb. 0.8-kb, and 0.6-kb *Hin*dIII fragments, (iii) 2.6-kb, and 1.5-kb *Cla*I fragments, and (iv) 2.2-kb *Eco*RI fragment. The 3.8-kb *Xba*I fragment (G fragment) hybridized to the following fragments of pXO2 from the wild-type strains; i) 3.8-kb *Xba*I fragment, ii) 4.2-kb *Hin*dIII fragment, iii) 5.2-kb *Cla*I fragment, and iv) 1.8-kb and 1.5-kb *Eco*RI fragments. These results are shown in Table 18.

The fragments containing the *cap* structural genes hybridized to the corresponding *Hin*dIII fragments in the restriction map of pTE702 as reported by Uchida, et al. (22), and to the similar *Hin*dIII fragments depicted in Robertson's map of pXO2. The results from *Cla*I restriction and hybridization analysis conflict with Robertson's *Cla*I restriction map of pXO2. Our data suggested that the locations of the 2.6-kb and the 1.5-kb *Cla*I fragments should be inverted. These results were confirmed with the location of Tn*917* insertion in mutant tp40. Tp40 shows insertion of Tn*917* in the 0.8-kb *Hin*dIII fragment as well as in the 1.5-kb *Cla*I fragment. It would be impossible to map this insertion in Robertson's map of pXO2 since the 0.8-kb *Hin*dIII fragment and the 1.5-kb *Cla*I fragment do not overlap in that map. Once the position of these two fragments is inverted, the results are consistent with the map.

The labelled fragments from pUBCAP1 were also used in DNA-DNA hybridization experiments to probe some of the insertion mutants to determine whether tn*917* was located in any of the *cap* genes. In 2 out of 20 insertion mutants examined so far (tp7 and tp40), Tn*917* has been localized within the *cap* region. Two other mutants, tp6 and tp38, exhibit deletions of about 20 kb and 50 kb respectively. These deletions which include the *cap* region were probably mediated by Tn*917*.

Analysis of pXO2::Tn*917* from mutant tp24-17, a deletion derivative. Mutant tp24-17 has a deleted version of pXO2 which is approximately only 10.5 kb in size including the transposon. Tp24-17 makes smooth, but not mucoid, colonies when grown in the presence of bicarbonate and CO_2. However, the amount of capsular material produced (if the smooth phenotype is indeed a reflection of synthesis of capsular material) is much less than that observed for wild-type pXO2-containing strains. Evidence that this mutant synthesizes some component of the capsule comes from experiments with bacteriophage CP-54 which can not adsorb to encapsulated cells, allowing selection of encapsulated cells. Smooth colonies of tp24-17 appear after two days of incubation on plates spread with CP-54. Results from DNA-DNA hybridization experiments show that the mutant plasmid in tp24 does not contain any of the *cap* structural genes identified by Makino, et al. (7, 8). However, colonies of tp24-17 are more smooth than colonies of strain TE704 which is the strain containing the cloned *cap* structural genes in plasmid pUBCAP1. These results suggest that this plasmid may contain a structural gene encoding an additional component of the capsule.

Plasmid DNA from tp24-17 gives two new fragments upon digestion with *Eco*RI, a 7.8 kb fragment and a 2.7 kb fragment. These fragments were isolated by electroelution, labeled with digoxigenin-labeled dUTP, and used as probes in DNA-DNA hybridization experiments to (i) locate their origin on pXO2 from *B. anthracis* 4229 UM12, and (ii) detect any homology with pXO2 from *B. anthracis* 6602, plasmid DNA from strain TE702, and the cloned *cap* structural genes in pUBCAP1.

The fragments of pXO2 and pTE702 to which each of the probes hybridized are listed in Table 19. In summary, the 7.8-kb *Eco*RI fragment hybridized to the following fragments of pXO2 and pTE702 from

wild-type strains; (i) 6.3-kb and 4.2-kb *Eco*RI fragments, (ii) 13-kb *Hin*dIII fragment, (iii) 8.2-kb *Xba*I fragment. Similarly the 2.7-kb *Eco*RI fragment hybridized to the following fragments in pXO2 and pTE702 from wild-type strains; (i) 2.7-kb *Eco*RI fragment, (ii) 13-kb *Hin*dIII fragment, (iii) 8.5-kb *Xba*I fragment. No homology was found with the *cap* structural genes identified by Makino, et al. (7, 8).

Analysis of insertion mutants that appear to be polypeptide overproducers. We reported previously that some insertion mutants (tp49, tp50, and tp60) appear to be polypeptide overproducers. The stringy properties of their colonies, the confluent growth they form on agar plates, and the loss of capsular material in a short period of time resemble polypeptide production by *B. licheniformis*. Tn*917* has been shown by DNA-DNA hybridization experiments to be located in the chromosome of tp50 and in the capsule plasmid of tp49 and tp60. The phenotype of tp60 is different from that of tp49 and tp50 in that tp60 is CO_2-independent for synthesis of capsular material. However, it overproduces capsular material only when it is grown in the presence of CO_2. Restriction analysis of plasmid DNA from strains tp49 and tp60 show the same restriction pattern with insertion of Tn*917* within the same fragment. To determine whether the orientation of Tn*917* might account for the difference in these phenotypes, the orientation of Tn*917* was determined by probing the *Hin*dIII-digested plasmids with the *Ava*I arms of Tn*917*. The results show that Tn*917* is in the same orientation in pXO2 from both of these mutants.

Colonies of the mutants that are overproducers of glutamyl polypeptide are extremely mucoid and they spread over the agar surface much more than do colonies of the encapsulated wild-type. As noted above, the capsular material produced by the mutants appears to "dry up" after a rather short time of incubation. It appeared to us that the material was probably being degraded. This is characteristic of *B. licheniformis* strains which produce glutamyl polypeptide and which also produce a peptidase that hydrolyzes the peptide. This enzyme has not been shown to be produced by *B. anthracis*. However, results of further experiments have suggested another possibility. We observed that when cells were grown on top of a dialysis membrane spread over the agar surface, the capsular material was produced in large quantities but it did not "dry up" or disappear in the way that it appeared to when cells were grown directly on the agar surface. It now appears to us that in the overproducing mutants the capsular material is not "contained" in the same way that it is in wild-type cells, and it is therefore free to diffuse into the agar medium. However, when a dialysis membrane separates the cells from the agar surface, the material can not go through the membrane and thus persists on the surface. These observations and interpretations suggest that the capsule of wild-type *B. anthracis* contains more than glutamyl polypeptide.

Quantitative determination of glutamyl polypeptide produced by "overproducing" mutants. To conduct quantitative determinations on the composition and amount of capsular material produced by some of our interesting transposants of strain 4229 which have Tn*917* inserted in pXO2, it was desirable to have a synthetic medium that would support capsule formation and polypeptide synthesis to the extent

that many natural media do. Strain 4229 does not grow on minimal XO medium and it grows poorly on minimal IB, which is a suitable medium for growth of some strains. After testing a variety of additions to minimal IB, we arrived at the following medium which we designate medium IIIB. The composition in grams per liter is as follows:

Minimal IIIB

L-leucine	0.32	L-glutamic acid	0.40
L-valine	0.32	glycine	0.40
L-alanine	0.32	nicotinamide	0.01
L-serine	0.32	thiamine.HCl	0.01
L-threonine	0.32	glucose	5.0
L-proline	0.32	$(NH_4)_2SO_4$	2.0
L-phenylalanine	0.32	KH_2PO_4	6.0
L-glutamine	0.32	K_2HPO_4	14.0
L-histidine	0.32	trisodium citrate	1.0
L-arginine	0.32	$MgSO_4.7H_2O$	0.4
L-isoleucine	0.32	$MnSO_4.H_2O$	0.05
L-asparagine	0.32	$CaCl_2.2H_2O$	0.15
L-methionine	0.32	$FeSO_4$	0.02

Dialysis membranes were placed on minimal IIIB-$NaHCO_3$ agar plates and three loopfuls of cells grown on $LPACO_3$ medium (for wild-type strain) and $LPACO_3$ containing erythromycin and lincomycin (for mutants) were spread on each of three plates. One set of three plates was incubated at 37°C in 20% CO_2 for 24 hours and another set was incubated under the same conditions for 48 hours. After incubation the membranes from three plates were removed from the agar surface with forceps, placed in a beaker containing 35 ml of distilled water, and autoclaved for 30 minutes at 121°C to extract the peptide. After autoclaving, the membranes were discarded and cells were removed by centrifugation. The supernatant samples were analyzed for glutamyl polypeptide by determining free glutamic acid (by paper chromatography) before and after acid hydrolysis (5, 21). Results from these experiments showed that the "overproducer" mutants did, in fact, produce considerably larger amounts of glutamyl polypeptide than did the parental wild-type strain. The averages of results from four experiments are shown in Table 20. Results are expressed as mg of glutamic acid per mg of cell dry weight.

Preliminary results of experiments to determine the proportions of L- and D-glutamic acid in the polypeptide indicate that greater than 90% of the glutamic acid released upon acid hydrolysis of

preparations from the wild-type parent strain, as well as from the overproducing mutants, is comprised of the D-isomer.

B. anthracis 4229 UM12 (carrying wild-type pXO2) as well as insertion mutants tp49, tp50, and tp60 grow well on minimal IIIB and all four strains produce capsules on minimal IIIB agar containing bicarbonate and incubated in CO_2. However, tp60 which is CO_2 independent for capsule synthesis on rich media such as LPA, is not capsulated when grown on minimal IIIB in the absence of added bicarbonate and CO_2. We tested each component of minimal IIIB individually to determine whether capsule synthesis by tp60 grown on minimal IIIB agar in air was inhibited by any of them. None of the components was found to be inhibitory. Thus, it appears that LPA medium contains something, not present in minimal IIIB, that promotes capsule synthesis by tp60 in the absence of added bicarbonate and CO_2. A large number of compounds including vitamins, amino acids, purines, and pyrimidines, have been tested but thus far none has been found to be effective in promoting capsule synthesis on minimal IIIB in the absence of bicarbonate and CO_2. This phenotype appears to be particular to tp60 since other mutants that are Cap^+ in air on LPA agar medium are also Cap^+ in minimal IIIB agar medium when incubated in air.

IV. Investigation of phage TP-21 whose prophage is a plasmid

We have shown that the 46-kb plasmid of Bacillus thuringiensis subsp. kurstaki strain HD-1 is the prophage of a phage which we have named TP-21 (12-14, 17, 18). This appears to be the first phage with a plasmid prophage described for the genus *Bacillus*. We have shown that TP-21 is a generalized transducing phage. It is likely that some of the transfer of genetic material attributed by other workers to conjugation-like processes in this strain is the result of TP-21-mediated transduction. TP-21 plaque-forming particles contain greater than 48 kilobase pairs of DNA which appears to be circularly permuted and terminally redundant. We isolated TP-21 lysogens which have the 5.2-kb MLS resistance transposon Tn*917* inserted in the prophage. Although insertion of Tn*917* rendered some isolates defective, several isolates carrying this element produced viable phage which confer erythromycin resistance upon lysogenized hosts. Results of tests with TP-21::Tn*917* demonstrate a broad host range among *B.anthracis*, *B.cereus* and *B.thuringiensis* strains.

TP-21 lysogens were very stable during growth at high temperatures. A mutant of TP-21, TP-21*c7*, was isolated following nitrosoguanidine mutagenesis of a *B.anthracis* lysogen; this derivative appears to be temperature sensitive for replication. *B. cereus* lysogens of TP-21*c7* grown at 30oC stably maintain the plasmid prophage. At 42^{o}C strains apparently cured of TP-21*c7* could be isolated from broth cultures grown from lysogens. A derivative of TP-21*c7* was isolated which has Tn*917* inserted. Lysogens of the transposon-tagged derivative, like those of the parental mutant phage, were stable at 30^{o}C but apparently

could be cured of the prophage at 42°C. For many reasons TP-21c7::Tn*917* seemed as if it should serve as an ideal transposition selection vector. However, several experiments in which it was tested as a mutagenic vehicle were unsuccessful. The reasons for this were not clear.

However, results of experiments during this reporting period have shown that the temperature-sensitive mutant of TP-21 which is tagged with Tn*917* mutates to defective forms during the curing procedure at 42°C in the presence of erythromycin and lincomycin. Thus, colonies that appeared to be transposants, i.e., ones that retained MLS resistance and seemed to be cured of TP-21 because they produced no lysis when planted in indicator lawns, were not transposants. Instead they harbored defective mutants of TP-21 which retained Tn*917*. Electrophoretic gels of plasmid extracts of presumed transposants revealed defective prophage plasmids of various sizes. Because the presence of erythromycin and lincomycin during the curing procedure apparently selects for phage mutants that are not temperature sensitive for replication, we carried out some experiments in which the curing procedure was done without selection for antibiotic resistance. These experiments, however, were unsuccessful. The frequency of MLS^r colonies that were cured of TP-21 was too low for this procedure to be useful for transposon mutagenesis. We have discontinued work on this problem so that we might put our full effort into studying the biology of the *B. anthracis* plasmids pXO1 and pXO2. It is conceivable, however, that we will do some work on TP-21 in the future if time permits.

Literature cited

1. **Battisti, L., B. D. Green, and C. B. Thorne.** 1985. Mating system for transfer of plasmids among *Bacillus anthracis*, *Bacillus cereus*, and *Bacillus thuringiensis*. J. Bacteriol. **162**:543-550.
2. **Green, B. D., L. Battisti, T. M. Koehler, C. B. Thorne, and B. E. Ivins.** 1985. Demonstration of a capsule plasmid in *Bacillus anthracis*. Infect. Immun. **49**:291-297.
3. **Hornung, J. M., A. I. Guaracao-Ayala, and C. B. Thorne.** 1989. Transposon mutagenesis in *Bacillus anthracis*. Abstr. H-256, p. 212. Abstr. 89th Annu. Meet. Am. Soc. Microbiol. 1989.
4. **Hornung, J. M., and C. B. Thorne.** 1991. Insertion mutations affecting pXO1-associated toxin production in *Bacillus anthracis*. Abstr. D-121, p. 98. Abstr. 91st Annu. Meet. Am. Soc. Microbiol. 1991.
5. **Leonard, C. G., R. D. Housewright, and C. B. Thorne.** 1958. Effects of some metallic ions on glutamyl polypeptide synthesis by *Bacillus subtilis*. J. Bacteriol. **76**:499-503.
6. **Leppla, S.** 1991. Purification and characterization of adenylyl cyclase from *Bacillus anthracis*. Methods Enzymol. **195**:153-168.

7. **Makino, S., C. Sasakawa, I. Uchida, N. Terakado, and M. Yoshikawa.** 1988. Cloning and CO_2-dependent expression of the genetic region for encapsulation from *Bacillus anthracis*. Mol. Microbiol. 2:371-376.

8. **Makino, S.-I., I. Uchida, N. Terakado, C. Sasakawa, and M. Yoshikawa.** 1989. Molecular characterization and protein analysis of the *cap* region, which is essential for encapsulation in *Bacillus anthracis*. J. Bacteriol. 171:722-730.

9. **Matson, S.** 1989. Suggestions and comments from sequencers, p. 18 Editorial comments. Vol. 16. United States Biochemical Corporation, Cleveland, OH.

10. **Robertson, D. L., T. S. Bragg, S. Simpson, R. Kaspar, W. Xie, and M. T. Tippetts.** 1990. Mapping and characterization of the *Bacillus anthracis* plasmids pXO1 and pXO2, p. 55-58. *In* P. C. B. Turnbull (ed.), Proceedings of the International Workshop on Anthrax, Winchester, England. Salisbury Medical Bulletin, No. 68, Special Supplement. Salisbury Medical Society, Salisbury, England.

11. **Robillard, N. J.** 1984. Changes associated with plasmid loss in *Bacillus anthracis*, Ph. D. Dissertation. University of Massachusetts, Amherst.

12. **Ruhfel, R. E.** 1989. Physical and genetic characterization of the *Bacillus thuringiensis* subsp. *kurstaki* HD-1 extrachromosomal temperate phage TP-21, Ph.D. Dissertation. University of Massachusetts, Amherst.

13. **Ruhfel, R. E., and C. B. Thorne.** 1988. Physical and genetic characterization of the *Bacillus thuringiensis* subsp. *kurstaki* HD-1 extrachromosomal temperate phage TP-21. Abstr. H-4, p. 145. Abstr. 88th Annu. Meet. Am. Soc. Microbiol. 1988.

14. **Ruhfel, R. E., and C. B. Thorne.** 1989. Isolation of a temperature-sensitive replication mutant of phage TP-21 and a Tn*917*-tagged derivative. Abstr. H-211, p. 204. Abstr. 89th Annu. Meet. Am. Soc. Microbiol. 1989.

15. **Sambrook, J., E. F. Fritsch, and T. Maniatis.** 1989. Molecular cloning: a laboratory manual. Cold Spring Harbor Laboratory Press, Cold Spring Harbor, N.Y.

16. **Thorne, C. B.** 1985. Genetics of *Bacillus anthracis*, p. 56-62. *In* L. Leive, P. F. Bonventre, J. A. Morello, S. Schlesinger, S. D. Silver, and H. C. Wu (eds.), Microbiology-1985. American Society for Microbiology, Washington, D.C.

17. **Thorne, C. B.** 1989. Genetic and physiological studies of *Bacillus anthracis* related to development of an improved vaccine. Annual Report, July 1989. Contract DAMD17-85-C-5212.

18. **Thorne, C. B.** 1990. Genetic and physiological studies of *Bacillus anthracis* related to development of an improved vaccine. Annual and Final Report, July 1990. Contract DAMD17-85-C-5212.

19. **Thorne, C. B.** 1993. *Bacillus anthracis*. In press. *In* J. A. Hoch, R. Losick, and A. L. Sonenshein (eds.), *Bacillus subtilis* and other gram-positive bacteria: physiology, biochemistry, and molecular genetics. American Society for Microbiology, Washington, D.C.

20. **Thorne, C. B., and F. C. Belton.** 1957. An agar diffusion method for titrating Bacillus *anthracis* immunizing antigen and its application to a study of antigen production. J. Gen. Microbiol. **17**:505-516.

21. **Thorne, C. B., C. G. Gomez, and R. D. Housewright.** 1952. Synthesis of glutamic acid and glutamyl polypeptide by *Bacillus anthracis* II. The effect of carbon dioxide on peptide production on solid media. J. Bacteriol. **63**:363-368.

22. **Uchida, I., K. Hashimoto, S.-I. Makino, C. Sasakawa, M. Yoshikawa, and N. Terakado.** 1987. Restriction map of a capsule plasmid of *Bacillus anthracis*. Plasmid **18**:178-181.

23. **Uchida, I., J. M. Hornung, C. B. Thorne, K. R. Klimpel, and S. H. Leppla.** Cloning and characterization of a gene whose product is a *trans*-activator of anthrax toxin synthesis. J. Bacteriol. In preparation.

24. **Welkos, S. L., J. R. Lowe, F. Eden-McCutchan, M. Vodkin, S. H. Leppla, and J. J. Schmidt.** 1988. Sequence and analysis of the DNA encoding protective antigen of *Bacillus anthracis*. Gene **69**:287-300.

25. **Youngman, P.** 1987. Plasmid vectors for recovering and exploiting Tn*917* transposition in *Bacillus* and other gram-positive bacteria, p. 79-103. *In* K. G. Hardy (ed.), Plasmids: a practical approach. IRL Press Ltd., Washington, D.C.

TABLE 1. Bacterial strains and plasmids used in this study

Strain	Relevant Characteristics	Plasmids	Source or reference
E. coli			
DH5α	*lacZ*ΔM15, r^-, m^+	none	(15)
DH5α(pBluescriptIIKS+)	Lac^+, Ap^r	pBluescriptIIKS+	T. G. Lessie
DH5α etf2-9.3	Lac^-, Ap^r	pBluescriptIIKS+ with 9.3-kb *Pst*I fragment from pXO1.1	This study
DH5α etf2-8.0	Lac^-, Ap^r	pBluescriptIIKS+ with 8.0-kb *Eco*RI fragment from pXO1.1	This study
DH5α etf3-8.0	Lac^-, Ap^r	pBluescriptIIKS+ with 5.8-kb *Eco*RI fragment from UM23 chromosome	This study
HB101(pSE42)	cloned *cya* on 7.4-kb *Bam*HI insert	pSE42	USAMRIID
JM103(pLF7)	cloned *lef*	pLF7	USAMRIID
B. anthracis			
Sterne (USAMRIID)	Tox^+, Cap^-	pXO1	C. B. Thorne
Weybridge	Tox^+, Cap^-	pXO1	C. B. Thorne
Weybridge A	Tox^+, Cap^-	pXO1	C. B. Thorne
Weybridge UM44-1	Ind^-, Tox^+, Str^r	pXO1	C. B. Thorne
Weybridge A UM23	Ura^-, Tox^+, PA^+, LF^+, EF^+,	pXO1.1	C. B. Thorne
Weybridge A UM23 tp1A	Ura^-, PA^+, LF^+, EF^+, MLS^r	pXO1.1::Tn*917*	This study
Weybridge A UM23 tp2A	Ura^-, PA^+, LF^+, EF^+, MLS^r	pXO1.1::Tn*917*	This study
Weybridge A UM23 tp20	Ura^-, PA^+, LF^+, EF^+, MLS^r	pXO1.1::Tn*917*	This study
Weybridge A UM23 tp21	Ura^-, PA^-, LF^+, EF^+, MLS^r	pXO1.1::Tn*917* deletion derivative	This study

Strain	Relevant Characteristics	Plasmids	Source or reference
Weybridge A UM23 tp27	Ura$^-$, PA$^+$, LF$^+$, EF$^+$, MLS^r	pXO1.1::Tn*917*	This study
Weybridge A UM23 tp28	Ura$^-$, PA$^+$, LF$^+$, EF$^+$, MLS^r	pXO1.1::Tn*917*	This study
Weybridge A UM23 tp29	Ura$^-$, PA$^-$, LF$^-$, EF$^-$, MLS^r	pXO1.1::Tn*917*	This study
Weybridge A UM23 tp29 tr1	Ura$^-$, MLS^r, Tc^r, Cry$^+$	pXO1.1::Tn*917*, pXO12::Tn*917*, pBC16	This study
Weybridge A UM23 tp32	Ura$^-$, PA$^-$, LF$^-$, EF$^-$, MLS^r	pXO1.1::Tn*917*	This study
Weybridge A UM23 tp36	Ura$^-$, PA$^+$, LF$^+$, EF$^+$, MLS^r	pXO1.1::Tn*917*	This study
Weybridge A UM23 tp39	Ura$^-$, PA$^-$, LF$^-$, EF$^-$, MLS^r	pXO1.1::Tn*917* deletion derivative	This study
Weybridge A UM23 tp39 etf3 and etf5	Ura$^-$, PA$^-$, LF$^+$, EF$^-$, MLS^r, Tc^r	pXO1.1::Tn*917*, pIU51	This study
Weybridge A UM23 tp40	Ura$^-$, PA$^+$, LF$^+$, EF$^+$, MLS^r	pXO1.1::Tn*917*	This study
Weybridge A UM23 tp49	Ura$^-$, PA^{++}, LF$^+$, EF$^{+/-}$, MLS^r	pXO1.1::Tn*917* deletion derivative	This study
Weybridge A UM23 tp56	Ura$^-$, PA$^-$, MLS^r	pXO1.1::Tn*917*	This study
Weybridge A UM23 tp62	Ura$^-$, PA^{a++}, LF^{a++}, EF^{a+}, MLS^r	pXO1.1::Tn*917*	This study
Weybridge A UM23 tp62C1 and tp62C2	Ura$^-$, Tox$^-$, MLS^s	(pXO1.1::Tn*917*)$^-$	This study
Weybridge A UM23 tp68	Ura$^-$, PA^{a+}, MLS^r	pXO1.1::Tn*917*	This study
Weybridge A UM23 tp70	Ura$^-$, PA$^-$, MLS^r	pXO1.1::Tn*917* deletion derivative	This study
Weybridge A UM23 tp71	Ura$^-$, PA$^{+/-}$, LF^{++}, EF$^+$, MLS^r	pXO1.1::Tn*917* deletion derivative	This study
Weybridge A UM23 tp72	Ura$^-$, PA$^{+/-}$, LF^{++}, EF$^+$, MLS^r	pXO1.1::Tn*917*	This study

Strain	Relevant characteristics	Plasmids	Source or reference
Weybridge A UM23 tp73	Ura$^-$, PA$^-$, MLS^r	pXO1.1::Tn*917* deletion derivative	This study
Weybridge A UM23 tp74	Ura$^-$, PA$^-$, MLS^r	pXO1.1::Tn*917* deletion derivative	This study
Weybridge A UM23C1	Ura$^-$	(pXO1.1)$^-$	C. B. Thorne
Weybridge A UM23C1-2	Ura$^-$, Rif^r	(pXO1.1)$^-$	C. B. Thorne
Weybridge A UM23C1-2 tr1-29	Ura$^-$, Tox$^-$, Rif^r, MLS^r, Cry$^+$	pXO1.1::Tn*917*^{b} pXO12::Tn*917*	This study
Weybridge A UM23C1-2 tr1-62 and tr4-62	Ura$^-$, Tox^{a+}, Rif^r, MLS^r, Cry$^+$	pXO1.1::Tn*917*^{b} pXO12::Tn*917*	This study
Weybridge B	Tox$^+$	pXO1	C. B. Thorne
Davis			
TE702	Cap^{c+}	pTE702	I. Uchida
TE704	Cap^{c+}	pUBCAP1	I. Uchida
Pasteur			
4229UM12	Cap^{c+}, Nal^r	pXO2	C.B. Thorne
4229UM12 tp1	Cap^{c+}, Nalr, MLS^r, Cm^s	pXO2::Tn917	This study
4229UM12 tp3	Cap^{c+}, Nal^r, MLS^r, Cm^s	pXO2::Tn917	This study
4229UM12 tp4	Cap^{c+}, Nal^r, MLS^r, Cm^s	pXO2::Tn917	This study
4229UM12 tp6	Cap$^-$, Nal^r, MLS^r, Cm^s	pXO2::Tn917	This study
4229UM12 tp7	Cap$^-$, Nal^r, MLS^r, Cm^s	pXO2::Tn917	This study
4229UM12 tp10	Cap^{c+}, Nal^r, MLS^r, Cm^s	pXO2::Tn917	This study
4229UM12 tp11	Cap^{c+}, Nal^r, MLS^r, Cm^s	pXO2::Tn917	This study
4229UM12 tp17	Cap^{c+}, Nal^r, MLS^r, Cm^s	pXO2::Tn917	This study

Strain	Relevant characteristics	Plasmids	Source or reference
4229UM12 tp18	Cap^-, Nal^r, MLS^r, Cm^s	pXO2::Tn917	This study
4229UM12 tp20	Cap^-, Nal^r, MLS^r, Cm^s	pXO2::Tn917	This study
4229UM12 tp21	Cap^-, Nal^r, MLS^r, Cm^s	pXO2::Tn917	This study
4229UM12 tp22	Cap^-, Nal^r, MLS^r, Cm^s	pXO2::Tn917	This study
4229UM12 tp24	Cap^{a+}, Nal^r, MLS^r, Cm^s	pXO2::Tn917	This study
4229UM12 tp24-17	Cap^{c+}, Nal^r, MLS^r, Cm^s	pXO2::Tn917	This study
4229UM12 tp30	Cap^{c+}, Nal^r, MLS^r, Cm^s	pXO2::Tn917	This study
4229UM12 tp38	Cap^-, Nal^r, MLS^r, Cm^s	pXO2::Tn917	This study
4229UM12 tp40	Cap^-, Nal^r, MLS^r, Cm^s	pXO2::Tn917	This study
4229UM12 tp49	Cap^{c++}, Nal^r, MLS^r, Cm^s	pXO2::Tn917	This study
4229UM12 tp58	Cap^{a+}, Nal^r, MLS^r, Cm^s	pXO2::Tn917	This study
4229UM12 tp59	$Capa^+$, Nal^r, MLS^r, Cm^s	pXO2::Tn917	This study
4229UM12 tp60	Cap^{a++}, Nal^r, MLS^r, Cm^s	pXO2::Tn917	This study
B. subtilis			
PA2	cloned *pag*	pPA102	USAMRIID
Plasmids			
pBluescriptIIKS+	2.9 kb, LacZα, Ap^r		T. G. Lessie
pIU51	cloned positive activating factor gene (*atxA*), Tc^r		(22)

(Table 1 continued next page)

(Table 1 continued)

[a] Abbreviations: USAMRIID, United States Army Medical Research Institute of Infectious Disease; Ap, ampicillin; MLS, macrolide, lincosamide, streptogramin B antibiotics; Tc, tetracycline; Rif, rifampicin; Ura, uracil; Ind, indole; Cry, crystal formation; Nal, nalidixic acid; Tox, toxin; PA, protective antigen; LF, lethal factor; EF, edema factor; *pag*, PA structural gene; *lef*, LF structural gene; *cya*, EF structural gene; ++, overproduction of the toxin component; a+, production of the toxin component in the presence or absence of added bicarbonate; *atxA*, positive *trans*-activator of toxin synthesis; Cap^{c+}, capsule production in presence of CO_2 and bicarbonate; Cap^{a+}, capulse production in air; Cap^{-}, inability to synthesize capsules; Cap^{c++}, overproduction of capsular material in the presence of CO_2 and bicarbonate.

[b] The two plasmids probably exist as a cointegrate.

TABLE 2. Restriction analysis of pXO1.1::Tn*917* derivatives from *B. anthracis* Weybridge A UM23 insertion mutants with *Pst*I and *Bam*HI

	*Pst*I fragments (kb)		*Bam*HI fragments (kb)		
pXO1.1::Tn*917* from	Altered	New[a]	Altered	New[a]	Altered Phenotypes[b]
UM23 tp56	ND[c]	ND	13.9	19.5	PA^-
UM23 tp68	6.6	11.8	34.8	39.8	PA^{a+}
UM23 tp70	18.1, 6.0	14.0	34.8, 13.9, 6.0	44.2	PA^-
UM23 tp72	6.0	11.4	6.0	11.4	PA^-
UM23 tp73	18.1, 6.0	14.0	34.8, 13.9, 6.0	44.2	PA^-
UM23 tp74	18.1, 6.0	14.0	34.8, 13.9, 6.0	44.2	PA^-

[a] The newly generated fragments were shown by DNA-DNA hybridization analysis to contain Tn*917*.

[b] PA^-, does not produce protective antigen; PA^{a+}, produces PA in the presence and absence of added bicarbonate.

[c] ND, not determined.

TABLE 3. Localization of Tn*917* within the altered *Bam*HI fragments of pXO1.1 from various insertion mutants by double digestion with *Bam*HI and *Sal*I

	*Bam*HI fragments (kb)		*Bam*HI-*Sal*I fragments (kb)		
pXO1.1::Tn*917* from	Altered	New	Altered	New[a]	Altered Phenotypes[b]
UM23 tp2A	34.8	39.8	34.8	30, 9.5[c]	none
UM23 tp20	14.6[d]	20	2.8	4.8, 3.5[c]	none
UM23 tp21	34.8, 13.9, 6.0	44.2	44.2	36[c], 8.5	PA^-, LF^+, EF^+
UM23 tp27	13.9	19.5	13.9	11.5, 7.6[c]	none
UM23 tp29	13.9	19.5	13.9	15[c], 4.5	PA^-, LF^-, EF^-
UM23 tp32	13.9	19.5	13.9	15[c], 4.5	PA^-, LF^-, EF^-
UM23 tp36	34.8	39.8	34.8	30, 9.5[c]	none
UM23 to39	34.8, 13.9, 7.4, 6.0	38.7	38.7	33[c], 5.5	PA^-, LF^-, EF^-
UM23 tp40	19.9[d]	25	6.0	8[c], 3.3	none
UM23 tp62	34.8	39.8	34.8	24[c], 15	PA^{a++}, LF^{a++}, EF^{a+}
UM23 tp68	34.8	39.8	34.8	32[c], 7.7	PA^{a+}
UM23 tp72	6.0	11.4	6.0	8.2[c], 3.2	PA^-

[a] The sizes of the *Bam*HI-*Sal*I restriction fragments are reported as approximate values.

[b] none, no changes in plasmid-associated phenotypes; PA, protective antigen; LF, lethal factor; EF, edema factor; $^-$, toxin component not detected; $^{++}$, overproduction of the toxin component; $^{a+}$, PA production in the presence or absence of added bicarbonate and CO_2.

[c] These *Bam*I-*Sal*I fragments were shown to hybridize to the 1.8-kb *Ava*I fragment (*erm* arm) of Tn*917*. The other fragments listed in this column without a superscript hybridized to the 2.2-kb *Ava*I fragment of Tn*917*.

[d] The 14.6-kb *Bam*HI fragment is cleaved by *Sal*I generating an 11.5-kb and a 2.8-kb fragment. The 19.9-kb *Bam*HI fragment is cleaved by *Sal*I generating a 13.9-kb and a 6.0-kb fragment (see Table 12).

TABLE 4. Protective antigen production by Weybridge A UM23 and UM23 tp62 grown in broth at 37°C with shaking

Medium[a]	PA production by[b]	
	UM23	UM23 tp62
CA + charcoal	<1	<1
CA	<1	4[c]
CA + charcoal + HS	1[c]	2[c]
CA + HS	<1	1[c]
CA + bicarbonate + charcoal	<1	<1
CA + bicarbonate	<1	<1
CA + bicarbonate + charcoal + HS	1	4
CA + bicarbonate + HS	1	2
CA(HEPES) + charcoal	4<8	>16<32
CA(HEPES)	<1	32
CA(HEPES) + charcoal + HS	8	>32<64
CA(HEPES) + HS	2	>32<64
CA(HEPES) + bicarbonate + charcoal	16	8
CA(HEPES) + bicarbonate	2	16
CA(HEPES) + bicarbonate + charcoal + HS	>16<32	>32<64
CA(HEPES) + bicarbonate + HS	>16<32	>32<64

[a] CA, casamino acids broth (pH 6.9); CA(HEPES), CA broth with 0.05 M HEPES (pH 7.5); +, an addition was made; charcoal, 4% Norit A was added to a final concentration of 0.2%; bicarbonate, 0.7% sodium bicarbonate was added; HS, heat-inactivated horse serum was added to a final concentration of 3%. The cultures were grown in 250-ml cotton-plugged flasks at 37°C for 15 h with slow shaking (100 rpm).

[b] PA from culture filtrates was detected by double immunodiffusion using goat antiserum to *B. anthracis* (provided by USAMRIID). The number reported represents the reciprocal of the highest dilution of the culture filtrate which produced a visible precipitin line.

[c] Partial line of identity with PA.

TABLE 5. Production of toxin components by *B. anthracis* Weybridge A UM23 and UM23 tp62 in CA-HEPES broth containing bicarbonate and horse serum

Filtrate[a]	PA Titer[b]		PA[c] μg/mg dry wt.		LF[c] μg/mg dry wt.		EF[c], μg/mg dry wt.	
	1	2	1	2	1	2	1	2
UM23, 8 h	8	4<8	17	16	9	5	2	3
UM23, 10 h	32	16<32	26	42	5	6	2	3
UM23, 12.5 h	64	32<64	49	46	26	9	5	6
UM23, 15 h	64	32<64	41	38	18	12	5	13
UM23, 17.5 h	32<64	32	46	43	14	12	1	12
UM23, 20 h	32<64	32	52	56	22	19	10	13
tp62, 8 h	4<8	8<16	16	30	8	6	1	3
tp62, 10 h	16<32	16<32	65	63	7	9	3	4
tp62, 12.5 h	>64	>64	84	73	32	14	7	9
tp62, 15 h	>64	32<64	80	61	34	23	7	19
tp62, 17.5 h	32<64	32<64	85	67	37	31	4	27
tp62, 20 h	64	32<64	92	78	28	32	15	18

[a] *B. anthracis* UM23 and UM23 tp62 were grown in casamino acids (CA)-0.05 M HEPES broth (pH 7.5) supplemented with 0.72% bicarbonate and 3% horse serum. Cultures were grown in 250-ml screw-capped flasks at 37°C with slow shaking (100 rpm) for the number of hours given. A flask was set up for each time point. The filtrates were obtained by mixing 10 ml of culture at various time points with 0.5 ml of horse serum and filtering the mixture through an HA membrane.

[b] PA in culture filtrates was detected by double immunodiffusion using goat antiserum to *B. anthracis*. The number reported represents the reciprocal of the highest dilution of culture filtrate that produced a visible precipitin line.

[c] PA and LF were determined by radial immunodiffusion using PA antiserum (goat) or LF antiserum (rabbit). EF was determined by adenylate cyclase assays. All concentrations are expressed as μg/mg of cell dry weight. 1, Experiment 1; 2, Experiment 2.

TABLE 6. Production of toxin components by *B. anthracis* Weybridge A UM23 and UM23 tp62 in CA-HEPES broth without bicarbonate and horse serum

Filtrate[a]	PA Titer[b]		PA[c] μg/mg dry wt.		LF[c] μg/mg dry wt.		EF[c] μg/mg dry wt.	
	1	2	1	2	1	2	1	2
UM23, 8 h	ND[e]	1	ND	4	ND	1	ND	<0.5
UM23, 10 h	2	4	3	4	0.5	<0.7	<0.3	<0.2
UM23, 12.5 h	2<4	4<8	2	<5	0.6	0.7	<0.2	<0.2
UM23, 15 h	2<4	2	3	2	0.2	<0.3	<0.1	<0.1
UM23, 17.5 h	1	<1	2	1	<0.2	<0.3	<0.1	<0.1
UM23, 20 h	<1	<1	0.4	0.5	<0.2	<0.3	<0.1	<0.1
UM23, 22.5 h	<1	<1	<0.4	<0.3	<0.2	<0.3	<0.1	<0.1
UM23, 25 h	<1	ND	<0.4	ND	<0.2	ND	<0.1	ND
tp62, 8 h	ND	4	ND	16	ND	2	ND	<1
tp62, 10 h	8<16	16	4	>11	2	4	2	2
tp62, 12.5 h	16	64	54	42	4	4	2	3
tp62, 15 h	64[d]	32	41	46	3	4	2	2
tp62, 17.5 h	64[d]	32[d]	43	35	2	>3	1	2
tp62, 20 h	16[d]	16[d]	32	28	3	>3	<0.1	<1
tp62, 22.5 h	8[d]	8[d]	9	>3	3	3	<0.1	<1
tp62, 25 h	8[d]	ND	9	ND	4	ND	<0.1	ND

[a] Same as for Table 5 except that cultures were grown in CA-HEPES broth (pH 7.5) without bicarbonate or horse serum.
[b] Same as for Table 5.
[c] Same as for Table 5.
[d] More than one precipitin band was observed suggesting the presence of degraded products.
[e] ND, not determined.

TABLE 7. Production of toxin components by *B. anthracis* Weybridge A UM23 and UM23 insertion mutants grown in the presence and absence of added bicarbonate and horse serum

Filtrate[a]	CA-HEPES with bicarbonate and horse serum[b]			CA-HEPES without bicarbonate and horse serum[b]		
	PA, ug/mg dry wt.	LF concn, ug/mg dry wt.	EF concn, ug/mg dry wt.	PA concn, ug/mg dry wt.	LF concn, ug/mg dry wt.	EF concn, ug/mg dry wt.
UM23	40 ± 5	12 ± 1	12 ± 6	2	<0.3	<0.1
UM23C1	<0.3	<0.3	<0.1	<0.3	<0.3	<0.1
UM23 tp1A	35 ± 6	12 ± 4	9 ± 4	2	<0.3	<0.1
UM23 tp2A	40 ± 7	11 ± 1	8 ± 3	2	<0.3	<0.1
UM23 tp20	39 ± 7	10 ± 2	9 ± 4	2	<0.3	<0.1
UM23 tp21[c]	<0.3	19 ± 3	19 ± 6	<0.3	1	<0.1
UM23 tp27	31 ± 2	10 ± 2	6 ± 2	1	<0.3	<0.1
UM23 tp28	33 ± 4	10 ± 2	5 ± 3	2	<0.3	<0.1
UM23 tp29	<0.3	<0.3	<1	ND[d]	ND	ND
UM23 tp32	<0.3	<0.3	<1	<0.3	<0.3	<0.1
UM23 tp36	38 ± 3	11 ± 2	6 ± 3	1	<0.3	<0.1
UM23 tp39[c]	<0.3	<0.3	<0.1	<0.3	<0.3	<0.1
UM23 tp40	35 ± 6	11 ± 2	6 ± 3	2	<0.3	<0.1
UM23 tp49[c]	67 ± 13	22 ± 4	1 ± 1	2	<0.2	<0.1
UM23 tp62	81 ± 12	27 ± 7	13 ± 2	48	3	1
UM23 tp71[c]	1 ± 1	65 ± 11	5 ± 2	<0.3	>3	<0.1
UM23 tp72	2 ± 2	27 ± 6	15 ± 3	0.4	>4	1

[a] Culture conditions are described in Table 5. Filtrates were collected from cultures grown for 13 h in broth supplemented with bicarbonate and horse serum or for 14 h in broth without bicarbonate and horse serum.

[b] See Table 5, footnote c. The values obtained for the concentrations of PA, LF, and EF in the filtrates from cultures grown in the presence of added bicarbonate and horse serum are the averages from three experiments.

[c] These insertion mutants contain deletions within pXO1.1::Tn*917* derivatives ranging from 16 to 150 kb.

[d] ND, not determined.

TABLE 8. Protective antigen production by Weybridge A UM23 tp29 and tp62 derivatives

Strain[b]	PA Production[a]	
	Medium A	Medium B
UM23 (pXO1.1)$^+$	32	4<8
UM23C1 (pXO1.1)$^-$	<0.1[c]	<1
UM23 tp62	32<64	32
UM23C1-2 tr1-62	ND[d]	32
UM23C1-2 tr4-62	ND	32
UM23 tp62C1	<1	ND
UM23 tp62C2	<1	ND
UM23 tp29	<0.1[c]	ND
UM23C1-2 tr1-29	<0.1[c]	ND

a Medium A, Casamino acids-0.05 M HEPES (CA-HEPES) broth (pH 7.5) containing 0.72% sodium bicarbonate, 3% horse serum, and 0.2% Norit A; Medium B, CA-HEPES containing only Norit A. Cultures were grown in 250-ml cotton-plugged flasks at 37°C for 15 h with slow shaking (100 rpm). PA from culture filtrates was detected by double immunodiffusion using goat antiserum to *B. anthracis* (provided by USAMRIID). The value reported represents the reciprocal of the highest dilution of the culture filtrate which produced a visible precipitin line.

b tr, denotes transcipient.

c The cultures filtrates were lyophilized and resuspended in gelatin-phosphate diluent to one-tenth the original volume.

d ND, not determined.

TABLE 9. Location of toxin structural genes on pXO1.1::Tn*917* deletion derivatives

Probe[a]	Hybridization to *Bam*HI fragments (kb) from					Hybridization to *Pst*I fragments (kb) from				
	pXO1.1	tp21[b]	tp39[b]	tp49[b]	tp71[b]	pXO1.1	tp21[b]	tp39[b]	tp49[b]	tp71[b]
*Eco*RI fragments from pLF7 (LF gene)	34.8	44.2[c]	39.8[c]	40c		6.6 6.0	14.0[c] 6.6	7.2[c] 6.6	6.6 6.0	16.0[c] 6.6
7.4-kb *Bam*HI fragment from pSE42 (EF gene)	7.4	7.4	39.8[c]	-[d]	-	18.7 5.5	18.7 5.5	18.7 7.2[c]	-	-

[a] The probes were labelled with digoxigenin-dUTP by random primer labelling.

[b] *Bam*HI and *Pst*I fragments were generated from digestion of pXO1.1::Tn*917* deletion derivatives isolated from tp21, tp39, tp49, and tp71.

[c] These fragments contain Tn*917*.

[d] -,the probe did not hybridize to any major fragments.

Table 10. Restriction analysis of the *Bam*HI and *Pst*I fragments located within the toxin-encoding region of pXO1.1 (Weybridge A UM23)

pXO1.1 fragment[a]	Restriction enzyme used for second digestion[b]	Restriction fragments generated from second digestion (kb)
34.8-kb *Bam*HI fragment	*Pst*I	9.3, 6.6, 6.3, 5.2, 4.7
18.7-kb *Pst*I fragment	*Bam*HI	14.6, 2.7[c], 2.0[c]
18.1-kb *Pst*I fragment	*Bam*HI	13.9, 4.8[c]

[a] pXO1.1 from Weybridge A UM23 was digested with *Bam*HI or *Pst*I. Following electrophoresis on an agarose gel, the restriction fragments were eluted from the gel and precipitated with one-tenth volume of 3 M sodium acetate (pH 5.2) and 2 volumes of 100% ethanol. The DNA was collected by centrifugation and the final DNA pellet was resuspended in TE (100 mM Tris-HCl, 1 mM EDTA, pH 8.0)

[b] The isolated fragments from pXO1.1 were then digested with either *Pst*I or *Bam*HI.

[c] These restriction fragments did not comigrate with any *Bam*HI or *Pst*I restriction fragments from pXO1.1.

TABLE 11. Location of toxin structural genes on pXO1.1 from Weybridge A UM23 and pXO1 from Sterne (USAMRIID)

Probe[a]	Hybridization to *Bam*HI fragments (kb) from pXO1		Hybridization to *Pst*I fragments (kb) from pXO1	
	Sterne[b]	UM23[b]	Sterne[b]	UM23[b]
2.2-kb *Eco*RI fragment from pPA102 (PA gene)	6.0	6.0	6.0	6.0
*Eco*RI fragments from pLF7 (LF gene)	29	34.8	6.6, 6.0	6.6, 6.0
7.4-kb *Bam*HI fragment from pSE42 (EF gene)	7.4	7.4	8.6, 5.5	18.7, 5.5

a The probes were labelled with digoxigenin-dUTP by random primer labelling.

b *Bam*HI and *Pst*I fragments were generated by digestion of pXO1 isolated from *B. anthracis* Sterne (USAMRIID) or pXO1.1 isolated from *B. anthracis* Weybridge A UM23.

TABLE 12. *Bam*HI and *Bam*HI-*Sal*I restriction profiles of pXO1.1 from Weybridge A UM23 and pXO1 from *B. anthracis* Sterne (USAMRIID)

*Bam*HI fragments (kb) from[a]		*Bam*HI-*Sal*I fragment (kb) from[a]	
pXO1.1 (Weybridge A UM23)	pXO1 (Sterne)	pXO1.1 (Weybridge A UM23)	pXO1 (Sterne)
38.7	38.7		
34.8		**34.8**	
		32	32
	29		
26.2	26.2	26.2	26.2
			26.2
19.9	19.9		
	19.5		**19.5**
14.6			
13.9	13.9	13.9	13.9
		13.9	13.9
		11.5	
7.7	7.7	7.7	7.7
7.4	7.4	7.4	7.4
7.1	7.1	7.1	7.1
		6.7	6.7
6.6	6.6	6.6	6.6
6.0	6.0	6.0	6.0
		6.0	6.0
3.9	3.9	3.9	3.9
		2.8	2.8

[a] The fragments shown in boldface represent differences observed in the restriction profiles of pXO1.1 (Weybridge A UM23) and pXO1 (Sterne). The underlined fragments are the *Bam*HI restriction fragments of the plasmids from Weybridge A UM23 and Sterne (USAMRIID) that contain *Sal*I restriction sites and the resulting *Bam*HI-*Sal*I restriction fragments of each plasmid.

TABLE 13. DNA-DNA hybridization analysis of the restriction fragments at the ends of the inverted region of pXO1 from Sterne (USAMRIID) and pXO1.1 from Weybridge A UM23

Probe[a]	Hybridization to *Pst*I fragment (kb) from pXO1		Hybridization to *Bam*HI fragments (kb) from pXO1	
	Sterne[b]	UM23[b]	Sterne[b]	UM23[b]
34.8-kb *Bam*HI fragment of pXO1.1 from Weybridge A UM23	19, 8.6, 6.6, 6.3, 6.0, 5.2	9.3, 6.6, 6.3, 6.0, 5.2	29, 19.5	34.8
14.6-kb *Bam*HI fragment of pXO1.1 from Weybridge A UM23	19	18.7	29	14.6
19-kb *Pst*I fragment of pXO1 from Sterne (USAMRIID)	19	18.7, 9.3	29, 7.7	34.8, 14.6, 7.7
8.6-kb *Pst*I fragment of pXO1 from Sterne (USAMRIID)	8.6	18.7, 9.3	19.5, 7.4	34.8, 7.4

a The fragments used as probes were electroeluted from gels and labeled with digoxigenin-labelled dUTP.

b *Pst*I and *Bam*HI fragments were generated from digestion of pXO1 isolated from Sterne (USAMRIID) or of pXO1.1 isolated from Weybridge A UM23.

TABLE 14. Phenotypic analysis of *B. anthracis* Sterne (USAMRIID) and Weybridge derivatives

Strain	pXO1-associated phenotypes			
	PA production[a]	Sporulation at 37°C[b]	Growth on minimal medium at 37°C[c]	CP-51 sensitivity[d]
Sterne (USAMRIID)	4	Spo^+	±	+
Weybridge	8	Spo^+	±	+[e]
Weybridge UM44-1	4	Spo^+	+	+
Weybridge A UM23	8	Osp^+	+++	-
Weybridge B	8	Spo^+	±	+[e]

[a] PA, protective antigen. Number denotes the reciprocal of the highest dilution of the culture filtrate which produced a visible precipitin line in the double immunodiffusion assay.

[b] Spo^+, extensive sporulation; Osp^+, oligosporogenous.

[c] Growth was reported as ± to +++ with ± representing poor growth and +++ representing extensive growth.

[d] +, plaque formation; -, no detectable plaques.

[e] Plaques were more turbid than that observed wih Sterne (USAMRIID) or Weybridge UM44-1.

TABLE 15. *Eco*RI restriction fragments altered by Tn*917* insertion within pXO2 from *B. anthracis* 4229 UM12 insertion mutants

Origin of plasmid[a]	*Eco*RI fragments (kb)[b]		Phenotype[e]
	Altered[c]	New[d]	
tp1	9.8	15.4	Cap^{c+}
tp3	6.3	11.9	Cap^{c+}
tp4	6.3	11.9	Cap^{c+}
tp6	-	7.8	Cap^{-}
tp7	2.2	6.3	Cap^{-}
tp10	4.6	10.2	Cap^{c+}
tp11	9.8	15.4	Cap^{c+}
tp17	7.8	13.4	Cap^{c+}
tp18	7.8	13.4	Cap-
tp20	7.8	13.4	Cap^{-}
tp21	6.3	11.9	Cap^{-}
tp22	4.2	9.8	Cap^{-}
tp24	6.3	11.9	Cap^{a+}
tp24-17	-	7.8, 2.7	$Cap^{c\pm}$
tp30	7.5	13.1	Cap^{c+}
tp38	-	10.5	Cap^{-}
tp40	2.2	5.7	Cap^{-}
tp49	6.3	8.2	Cap^{c++}
tp58	6.3	11.9	Cap^{a+}
tp59	5.8	11.4	Cap^{a+}
tp60	6.3	8.2	Cap^{a++}

[a] Insertion mutants whose parent strain is *B. anthracis* 4229 UM12.
[b] The restriction fragments are reported as approximate sizes.
[c] -, the altered fragment is unknown since these insertion mutants are deletants and more than one fragment is missing from the Tn*917*-tagged plasmids.
[d] These new fragments, except the 2.7-kb fragment from tp24-17, have been shown by DNA-DNA hybridizations to contain Tn*917*.
[e] Cap^{c+}, capsule production in presence of CO_2 and bicarbonate; Cap^{a+}, capsule production in air; Cap^{-}, inability to produce capsules; Cap^{c++}, overproduction of capsular material; $Cap^{c\pm}$, see text for phenotype of this mutant.

TABLE 16. *Hin*dIII restriction fragments altered by Tn*917* insertion in pXO2 from *B. anthracis* 4229 UM12 insertion mutants

Origin of plasmid[a]	*Hin*dIII fragments (kb)[b]		Phenotype[e]
	Altered[c]	New[d]	
tp3	13	8.9, 7.8, 1.3	Cap^{c+}
tp4	13	9.5, 6.8, 1.3	Cap^{c+}
tp6	-	10.2, 3.2, 1.3	Cap^{-}
tp7	6.6	6.9, 3.1, 1.3	Cap^{-}
tp10	3.4	4.6, 2.5, 1.3	Cap^{c+}
tp11	9.2	5.8, 5.6, 1.3	Cap^{c+}
tp17	4.05	6.6, 1.5, 1.3	Cap^{c+}
tp18	2.8	3.6, 3.2, 1.3	Cap^{-}
tp20	2.8	3.6, 3.2, 1.3	Cap^{-}
tp21	13	10.5, 6.5, 1.3	Cap^{-}
tp22	1.5	4.3, 1.3, 1.15	Cap^{-}
tp24-17	-	7.5, 1.7, 1.3	$Cap^{c\pm}$
tp30	3.3	3.9, 3.4, 1.3	Cap^{c+}
tp38	-	6.7, 6.5, 1.3	Cap^{-}
tp40	0.8	3.3, 1.5, 1.3	Cap^{-}
tp49	13	8.8, 4.4, 1.3	Cap^{c++}
tp58	13	8.7, 8.5, 1.3	Cap^{a+}
tp59	1.3	3.7, 1.6, 1.3	Cap^{a+}
tp60	13	8.8, 4.4, 1.3	Cap^{a++}

[a] Insertion mutants whose parent strain is *B. anthracis* 4229 UM12.
[b] The restriction fragments are reported as approximate sizes.
[c] -, the altered fragment is unknown since these insertion mutants are deletants and more than one fragment is missing from the Tn*917*-tagged plasmids.
[d] These new fragments have been shown by DNA-DNA hybridizations to contain Tn*917*.
[e] Cap^{c+}, capsule production in presence of CO_2 and bicarbonate; Cap^{a+}, capsule production in presence of air; Cap^{-}, inability to produce capsules; Cap^{c++}, overproduction of capsular material; $Cap^{c\pm}$, see text for description of this mutant.

TABLE 17. *Cla*I restriction fragments altered by Tn*917* insertion within pXO2 from *B. anthracis* 4229 UM12 insertion mutants

Origin of plasmid[a]	*Cla*I fragments (kb)[b]		Phenotype[e]
	Altered[c]	New[d]	
tp1	18	17, 2.1*, 1.5*, 1.1*	Cap^{c+}
tp3	10.5	7.9, 2.7, 2.1*, 1.5*, 1.1*	Cap^{c+}
tp4	10.5	7.8, 2.8, 2.1*, 1.5*, 1.1*	Cap^{c+}
tp6	-	22, 3.8, 2.1*, 1.5*, 1.1*	Cap^{-}
tp7	2.6	2.1*, 1.5*,1.1*	Cap^{-}
tp10	25	15, 11, 2.1*, 1.5*, 1.1*	Cap^{c+}
tp11	18	7.8, 8.0, 2.1*, 1.5*, 1.1*	Cap^{c+}
tp17	14	7.8, 6.2, 2.1*, 1.5*, 1.1*	Cap^{c+}
tp18	14	8.5, 5.5, 2.1*, 1.5*, 1.1*	Cap^{-}
tp20	14	8.5, 5.5, 2.1*, 1.5*, 1.1*	Cap^{-}
tp21	10.5	9.5, 2.1*, 1.5*, 1.1*	Cap^{-}
tp22	10.5	9.8, 2.1*, 1.5*, 1.1*, 0.8	Cap^{-}
tp24-17	-	5.2, 2.1*, 1.5*, 1.1*, 0.6	$Cap^{c\pm}$
tp30	25	22, 3.4, 2.1*, 1.5*, 1.1*	Cap^{c+}
tp38	-	2.8, 2.1*, 1.5*, 1.3, 1.1*	Cap^{-}
tp40	1.5	2.1*, 1.5*, 1.2, 1.1*	Cap^{-}
tp49	10.5	7.8, 2.1*, 1.5*, 1.1*	Cap^{c++}
tp58	10.5	9.2, 2.1*, 1.5*, 1.1*	Cap^{a+}
tp59	6.2	6, 2.1*, 1.5*, 1.1*	Cap^{a+}
tp60	10.5	7.8, 2.1*, 1.5*, 1.1*	Cap^{a++}

a Insertion mutants whose parent strain is *B. anthracis* 4229 UM12.

b The restriction fragments are reported as approximate sizes.

c -, the altered fragment is unknown since these insertion mutants are deletants and more than one fragment is missing from the Tn*917*-tagged plasmids.

d *, these new fragments have been shown by DNA-DNA hybridizations to contain Tn*917*.

e Cap^{c+}, capsule production in presence of CO_2 and bicarbonate; Cap^{a+}, capsule production in presence of air; Cap^{-}, inability to produce capsules; Cap^{c++}, overproduction of capsular material; $Cap^{c\pm}$, see text for description of this mutant.

TABLE 18. Location of the capsule structural genes in pXO2

Probe[a]	Hybridization to fragments (kb)[b]		
	*Xba*I	*Hin*dIII	*Cla*I
2.5-kb *Xba*I fragment from pUBCAP1	2.5	6.6, 4.2, 0.8	2.6, 1.5
3.8-kb *Xba*I fragment from pUBCAP1	3.8	4.2	5.2

[a] The 3.8-kb and 2.5-kb *Xba*I fragments from pUBCAP1 contain the *cap* structural genes. These fragments were labelled with digoxygenin-labelled dUTP and used as probes in DNA-DNA hybridizations with digested pXO2.

[b] The sizes of fragments were estimated. Plasmid DNA from wild-type strains TE702, 4229UM12 and 6602 was digested with *Xba*I, *Hin*dIII, or *Cla*I. All strains showed the same restriction profile and hybridization occurred to the same fragments in every case.

TABLE 19. Origin of fragments in the deletion derivative carried by tp24-17

Probe[a]	Hybridization to fragments (kb)[b]		
	*Eco*RI	*Hin*dIII	*Xba*I
7.8-kb *Eco*RI fragment from tp24-17	6.3, 4.2	13	8.2
2.7-kb *Eco*RI fragment from tp24-17	2.7	13	8.5

a The 7.8-kb and 2.7-kb *Eco*RI fragments from tp24-17 were labeled with digoxigenin-labelled dUTP and used as probes in DNA-DNA hybridizations with digested pXO2.

b Plasmid DNA from strains wild-type strains TE702, 4229UM12 and 6602 was digested with *Eco*RI, *Hin*dIII, or *Xba*I. All strains showed the same restriction profile and hybridization occurred to the same fragments in every case.

TABLE 20. Glutamyl polypeptide synthesis by *Bacillus anthracis* 4229 UM12 and insertion mutants tp49, tp50 and tp60[a]

Strain	Peptide as glutamic acid	
	at 24 hrs mg/mg cell dry weight	at 48 hrs mg/mg cell dry weight
4229 UM12	0.14	0.15
tp49	0.25	0.26
tp50	0.22	0.26
tp60	0.26	0.24

[a] Cells were grown on membranes placed on minimal IIIB-HCO_3 medium.

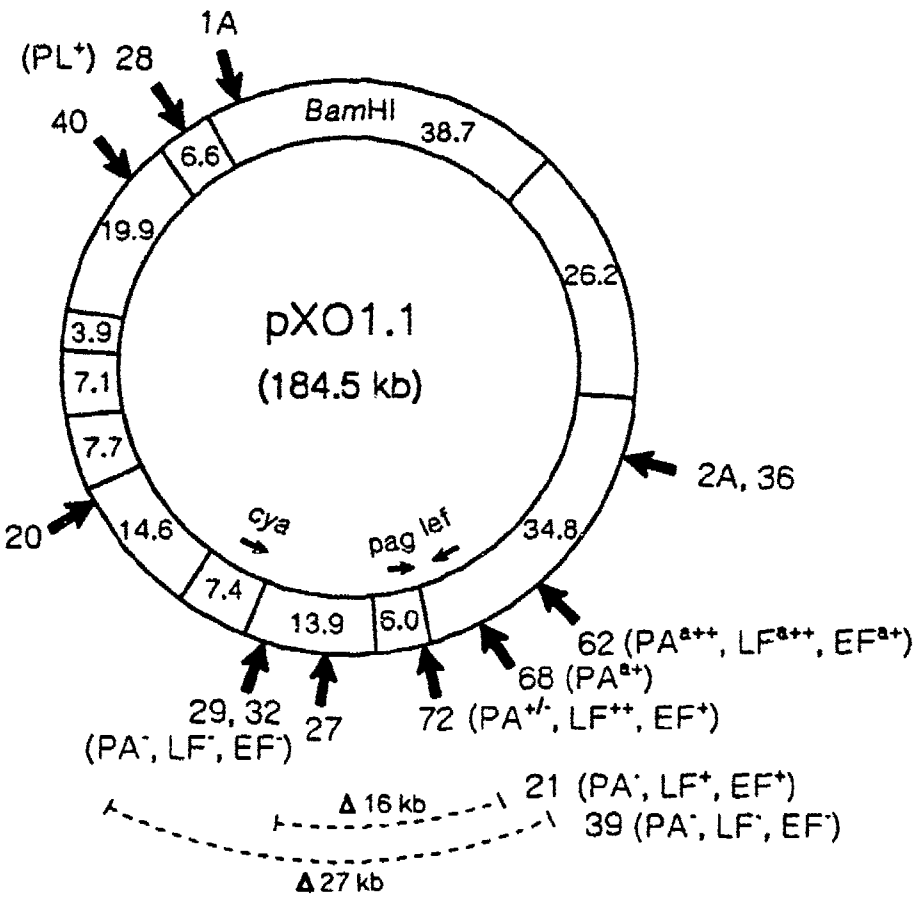

FIG. 1. Location of Tn*917* insertions on the *Bam*HI restriction map of pXO1.1 (Weybridge A UM23). The insertion mutants are designated as 1A to 72. The site of insertion of Tn*917* is shown by the arrow next to the insertion mutant number. Deletions are shown by a dotted line. Mutants with no phenotypic designations exhibit plasmid-associated phenotypes similar to those observed for the parent strain. PL$^+$, ability of bacteriophage CP-51 to form plaques on tp28; PA, protective antigen; LF, lethal factor; EF, edema factor; $^{++}$, overproduction; $^{a+}$, production of toxin components in the presence and absence of added bicarbonate.

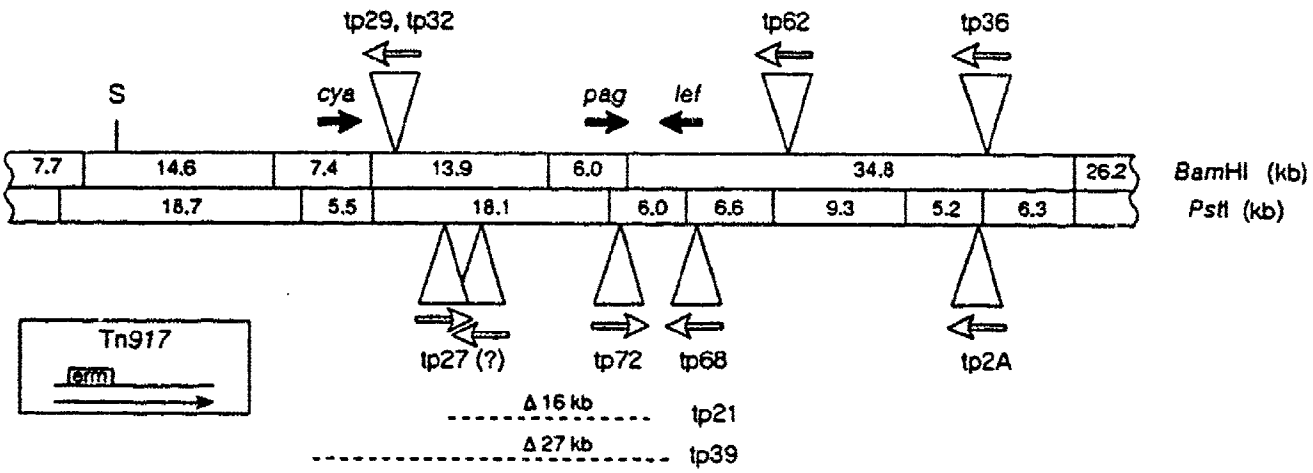

FIG. 2. Restriction map of pXO1.1 (Weybridge A UM23) toxin-encoding region showing the location and orientation of Tn*917* within the tagged plasmids from various insertion mutants. The location and direction of transcription of the toxin structural genes are indicated by the solid arrows. The open triangles show the site of insertion of Tn*917* on pXO1.1 from the insertion mutants listed above or below the triangles. The question mark next to tp27 indicates that Tn*917* insertion was localized to one of two regions within the 13.9-kb BamHI fragment. The open arrows show the orientation of Tn*917* with reference to that shown in the box. The deletions in the plasmids from tp21 and tp39 are shown by a dotted line. S, *Sal*I restriction site.

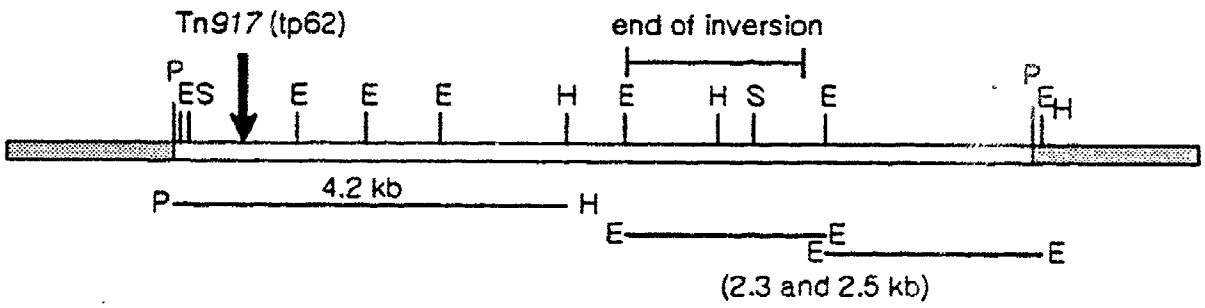

FIG. 3. Subcloning strategy of the 9.3 kb *Pst*I fragment of pXO1.1. The 4.2-kb *Pst*I-*Hin*dIII fragment contains the putative negative regulator of toxin synthesis. The arrow indicates the site of insertion of Tn*917* in pXO1.1 from tp62. One end of the inverted segment of the toxin-encoding region of pXO1.1 is located either on the 2.3-kb or the 2.5-kb *Eco*RI fragment. The fragments located below the 9.3-kb insert indicate those that will be subcloned. E, *Eco*RI; H, *Hin*dIII; P, *Pst*I; and S, *Sst*I. ▭, pBluescriptIIKS+; ▭, 9.3-kb *Pst*I fragment of pXO1.1.

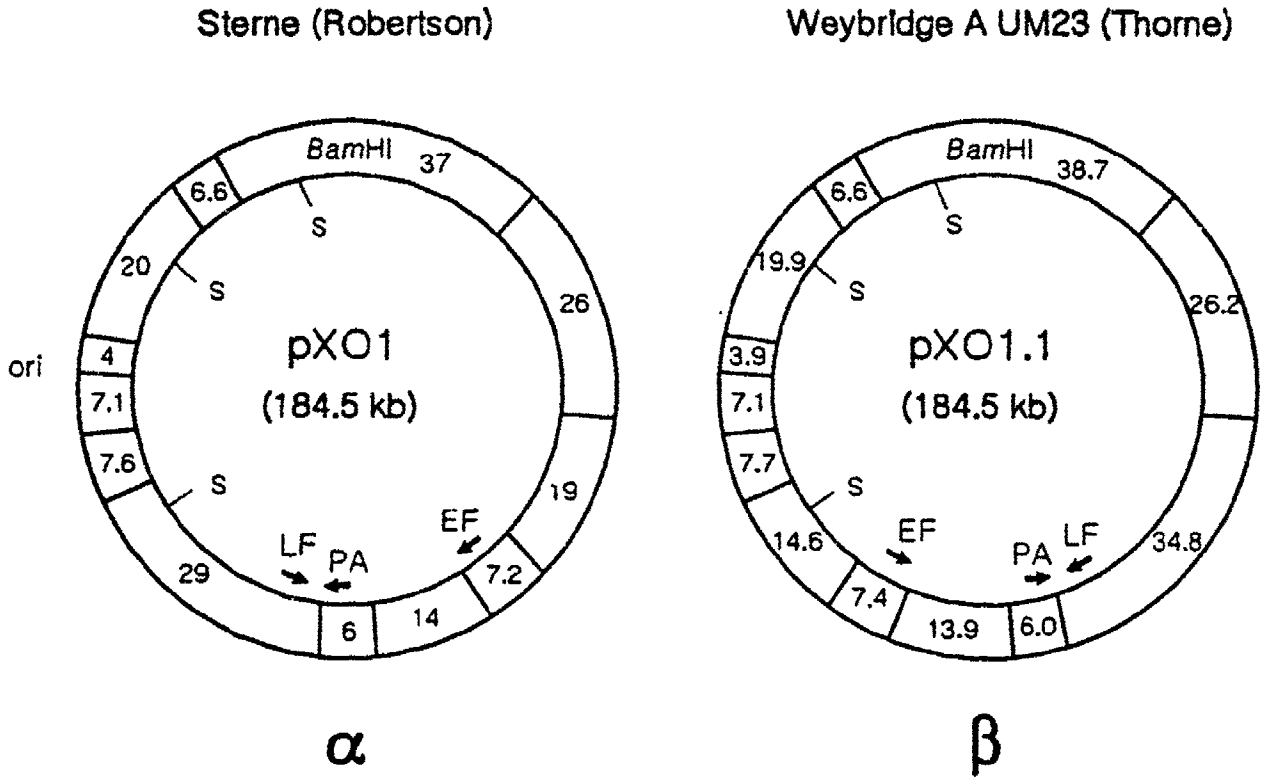

FIG. 4. Comparison of *Bam*HI restriction maps of the toxin plasmids. The map of pXO1 (Robertson) was constructed by Robertson *et al.* The map of pXO1.1 from Weybridge A UM23 was constructed based on data obtained from restriction analysis of pXO1.1, pXO1.1::Tn*917* derivatives, and deletion derivatives. The toxin-encoding region of pXO1 (Robertson) and pXO1.1 (Weybridge A UM23) is designated as being in the α or β orientations, respectively. S, *Sal*I restriction sites.

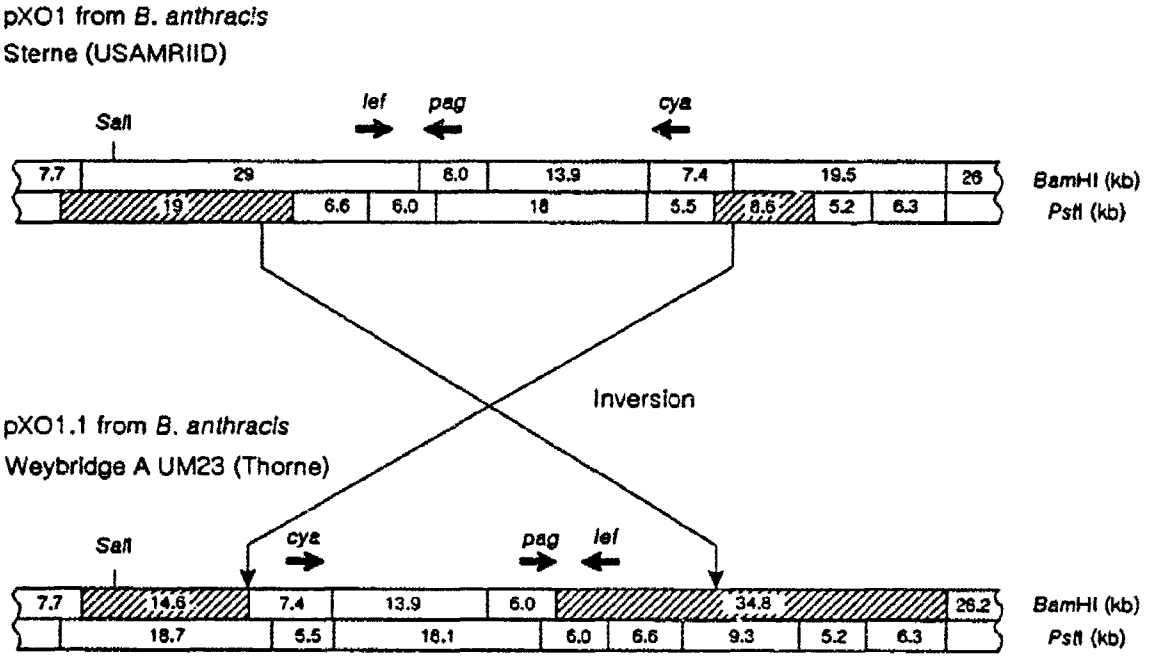

FIG. 5. Comparison of restriction maps of pXO1 toxin-encoding region. A 77-kb region of pXO1 encompassing the toxin structural genes is shown. Differences in restriction patterns of pXO1 from Sterne (USAMRIID) and pXO1.1 from Weybridge A UM23 are shown. The fragments shown with diagonal lines contain the ends of the inverted segment. These fragments were isolated and used in DNA-DNA hybridization analysis of the inversion. The region of pXO1 inverted represents approx. 40 kb.

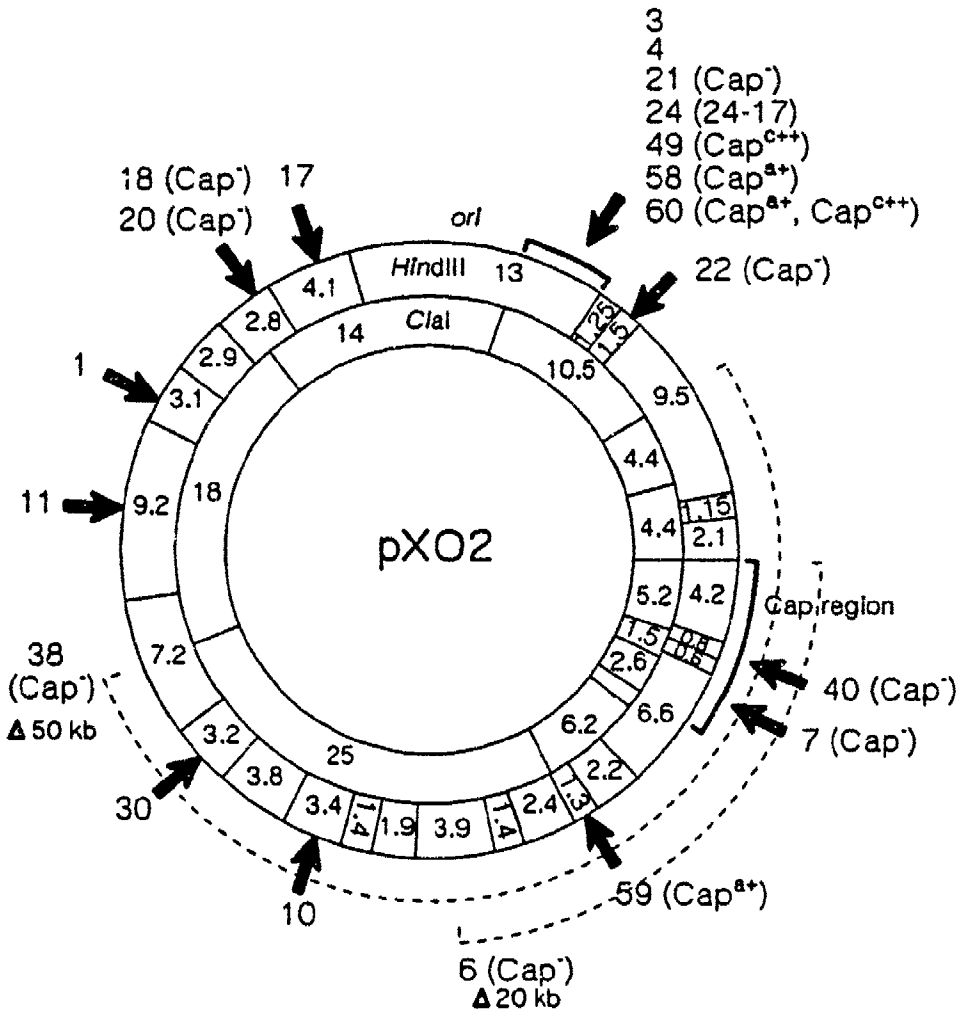

FIG. 6. Restriction map of pXO2. The locations of Tn*917* insertions are indicated by the arrows. Insertion mutants that exhibit the parental phenotype are not labeled with phenotypic designations. Deletions are indicated by dotted lines. Cap⁻, inability to produce capsule; Cap^{a+}, CO_2-independent for capsule production; Cap^{c++}, overproduction of capsular material in CO_2.